ISRN LUTMDN/TMHP-21/5470-SE

ISSN 0282-1990

The Wake Effect and Wind Farm Clustering

An assessment of wake effect impact on wind farm clusters in the Southern Middle Bank region

Igor Ciric

Master Thesis degree of Master of Science in Engineering
Division of Fluid Mechanics
Department of Energy Sciences
Faculty of Engineering | Lunds Universitet

The Wake Effect and Wind Farm Clustering

An assessment of wake effect impact on wind farm clusters in the Southern Middle Bank region

by Igor Ciric

LUND
UNIVERSITY

This degree project for the degree of Master of Science in Engineering has been conducted at the Division of Fluid Mechanics, Department of Energy Sciences, Faculty of Engineering, Lund University.

The supervisors at the Division of Fluid Mechanics were Robert-Zoltán Szász and Johan Revstedt. The examiner at Lund University was Professor Jens Klingmann.

Thesis for the Degree of Master of Science in Engineering

ISRN LUTMDN/TMHP-21/5470-SE

ISSN 0282-1990

Division of Fluid Mechanics

Department for Energy Sciences

Faculty of Engineering, Lunds University

Box 118, 221 00 Lund

Sweden

www.energy.lth.se

Preface

This master thesis was done out of a desire to learn more about the wake effect and its role for large scale offshore wind farms in the future. The work has been done at the department of energy sciences at LTH during the period October 2020 - May 2021. The master thesis marks the end of my time at Lund University and a life as a student.

I want to thank Robert-Zoltán Szász for his endless support during the whole time frame of the project. His support has shaped this work and without him this work wouldn't be possible. I also want to thank Johan Revstedt and Jens Klingmann for the supervision and help to initiate this project. It has been a pleasure to work with you all.

Finally, I would like to thank the technical support at *DNV GL* for their help to resolve any problems concerning the *Windfarmer: Analyst* software program.

Igor Ciric
Lund, May 2021

Abstract

The wind energy industry is growing rapidly and as offshore wind expands in the Baltic sea, more and more clusters will be observed. The purpose of this work is to better understand the impact that wakes have on the electricity production for wind farm clusters in the Southern Middle Bank region. This report aims to answer the following research questions; 1) How big of an impact do wakes have on electricity production for future wind farm clusters in the Southern Middle Bank region? 2) How do different changes made to the layout of the wind farm cluster impact the resulting electricity production change due to wakes? 3) What are the economical implications of making layout changes in order to mitigate the impact of the wake effect? In order to answer the research questions, the methodology was based on simulations done in the *WindFarmer: Analyst* software program (DNV GL, n.d.-a).

The results of this work has shown the importance of considering the wake effect for future offshore wind farm development. For clusters containing 20 turbines (16 MW), the lost electricity production due to wakes has been shown to stand for 4.8% of the gross yield when using 7D separation distance. When the separation distance was lowered to 4D, the loss of electricity production due to wakes stood for 14.1% of the gross yield.

Layout changes that were introduced in order to mitigate the impact of wakes, such as smaller rotor diameter and higher towers, showed modest improvements within the range of tenths of a percentage point. Other measures, such as sector management, resulted in a less desirable outcome. In the case of building neighbouring wind farm clusters (with a distance of ~3 km), the impact would be another 0.5 percentage points loss in electricity production relative to the gross yield. Therefore, key findings of this work are that it is most beneficial to build wind farms with larger separation distancing, both in terms of lowering the impact of wakes as well as profitability. However, this does not take into account how well the area is utilized or the total amount of electricity produced.

Table of Contents

1. Introduction

Wind power is among the fastest growing renewable energy technologies (IRENA, n.d.). At the same time as the usage is on the rise, the costs are falling. In the past two decades, the globally installed wind power capacity (both onshore and offshore) increased with a factor of almost 75, increasing from 7.5 GW in 1997 to 564 GW in 2018. Between 2009 and 2013, the electricity generated by wind power almost doubled and still, wind energy accounted for only 16% of the electricity generated by renewable energy sources in 2016.

As the competition over onshore sites has increased, there has been a bigger interest in building wind farms offshore (Eriksson, 2019). One of the advantages of building offshore wind farms is higher extraction of electricity due to higher wind speeds, but the building process is more complex and higher costs set additional risk. However, as the turbines get bigger in size, it is advantageous to place them offshore where they have a bigger potential because of the higher wind speeds. At the same time, finding a suitable site for an offshore wind farm may be a challenge.

In order to achieve higher profitability and lower the risks, it is favourable to choose an offshore site that has good conditions for the foundation but also for higher wind speeds (Eriksson, 2019). In order to achieve higher wind speeds, a site further away from the shore is usually chosen. However, such locations that at the same time are shallow in terms of water depth are not so abundant. This usually gives rise to a build-up of so-called clusters, where wind turbines are highly concentrated to a specific offshore area. Because of this, problems can arise when turbines are so closely placed that they start impacting each other. As the wind passes the turbine, a wake is created which results in reduced wind speed and increased turbulence for the turbines downstream. This has a negative impact on the electricity production within the wind farm but can also become a problem between two neighbouring wind farms.

As the occurrence of clusters is only expected to increase in the future, the observed negative impacts of wakes are also expected to be more common. This is due to the fact that future projects are being planned more closely located to each other than earlier (Eriksson, 2019). Therefore, it is highly relevant to study the impact of the wake effect. Especially when taking in consideration the goal from the European Union (RED II) to increase the target for the year 2030 with a 32% renewable energy penetration (European Commission, 2019).

This is relevant to the European Union as a whole, but especially to the region around the Baltic Sea, as the penetration of renewable energies are higher for some countries while others, such as Poland, is experiencing a very low renewable energy penetration being highly dependent on coal (Tillväxtanalys, 2014). Germany and Denmark are expected to be the biggest contributors, while Poland also will be in need to build offshore wind farms in order to comply with the Renewable Energy Directive (Hüffmeier & Goldberg, 2019). Finland has today a smaller share, about 71 MW (compared to Sweden's 172 MW) as it experiences environmental challenges with seasonal icing. Estonia, Lithuania and Latvia have only built a few test projects and 'on paper' the installed capacity is non-existent.

When constructing an offshore wind farm, it is usually done by a ‘maximise first’ strategy, where the maximization of produced electricity is a priority, and later the capital costs are considered for maximum profitability (EWEA, 2009). In one sense, the siting and planning phase is a way to predict wind speeds and electricity production in order to minimize uncertainties and risks. In the future, when more baltic countries decide to install offshore wind power, the current situation may contribute to realization of bigger wind farm projects that are very closely located. There is a high interest from different actors through the value chain to minimize the uncertainty of electricity production and generation loss. Taking into account that the obtained power is increasing with the cube of the wind speed for a wind turbine, evaluating losses due to wake effects can be of significant importance to minimize uncertainties (Manwell et al., 2009).

Therefore, it is highly interesting to study the impact of wake effects as an interaction between neighbouring wind farms (Eriksson, 2019). Better knowledge is needed of the resulting wind conditions that occur after the wake interaction between neighbouring wind farms, especially considering the impacts on electricity production. According to Eriksson (2019) a broad range of studies on the wake effect and the wake interaction within the wind farm has been done. However, Eriksson (2019) claims that the studies done on the resulting effects of the wakes between two wind farms are highly limited. The main difference is the distance in question, but the wake effects within a wind farm are also more dependent on the technical properties of the specific turbine while the bigger distance between wind farms provides an opportunity for the wind speeds to recover. Therefore, the impact resulting from wake effects between farms may be more dependent on other factors such as wind conditions bound to the location.

1.1 Background

The European Union has initiated the *Baltic Integrid* project in order to investigate the potential of a ‘meshed’ offshore grid system in the baltic sea (Avdic & Ståhl, 2019). The aim is to connect relevant stakeholders and optimize the offshore wind infrastructure. This will give rise to better grid connectivity between countries, but also formation of wind farm clusters. The regional meshed grid consists of HVDC transmission lines, and using the cluster formations as connection points for the grid in order to enable the possibility of cross-border electricity trade between countries. The advantages of such a system is a more efficient sharing of electricity due to the infrastructure but also due to the better matching of supply and demand.

1.1.1 Southern Middle Bank

The *Baltic InteGrid* project has identified some offshore areas that are well suitable for a build-out of bigger wind farm projects (Avdic & Ståhl, 2019). These areas are experiencing high wind speeds which are suitable for electricity production, but other aspects are also considered such as water depth, proximity to construction ports, distance to existing grid and visual impact. One such area is the Southern Middle Bank (SMB) Area. This region is explicitly selected because of the planned offshore wind projects in the area, which are planned in both the Polish exclusive economic zone (EEZ) and the Swedish EEZ. Many of these projects will be close to the border between these two, such as the two projects *Södra Midsjöbanken* and *Baltica-1* that were planned in the SMB region (Kullberg, 2011;

Naturvårdsverket, 2020). Suitable locations exist also in the Lithuanian EEZ, where the authorities already have reserved zones for future offshore projects.

Furthermore, submarine interconnections between Poland and Sweden and between Sweden and Lithuania (Nordbalt) already exist in the SMB region (Avdic & Ståhl, 2019). Another advantage of the region is that the area contains ~2000 km² of water shallower than 40 m and the distance to shore is relatively short, making it suitable for offshore wind farms. However, the region is too big for a single company to cover the whole area with turbines, so a scenario with cluster formation in the region is highly likely.

1.1.2 Farm to Farm Wakes

A few different simulation and measurement approaches have been used in order to estimate the impact of external wake effects between two wind farms (Eriksson, 2019). Although the results vary for every particular case, some general estimations have been obtained. For instance, measurements can be done based on wake measurements from satellite data, synthetic aperture radar (SAR) or by using Park and Eddy Viscosity models with a software program such as WASP (Eriksson, 2019). Furthermore, meso-scale models can be used, such as Meso-scale Flow with Wind Farming (MFwWF) which analyzes the interaction between a wind farm and the prevailing wind (Brand, 2009). However, the models have shown a big spread in results (Hansen et al., 2015). For instance, an estimation of the park efficiency for farm to farm wakes between Nysted and Rødsand II showed a spread between 10 and 15 percentage points for the different wake models, when the inflow direction was varied.

1.2 Aim

The aim of this work is to better understand the impact that wakes have on the electricity production for wind farm clusters in the SMB region. Therefore, a better knowledge of the impact of wakes within and in between wind farm clusters will be obtained. This will result in less uncertainties for future clustering of wind farms in the SMB region. The report aims to answer three specific research questions, namely;

Research Questions

1. How big of an impact do wakes have on electricity production for future wind farm clusters in the SMB region?

2. How do different changes made to the layout of the wind farm cluster impact the resulting electricity production change due to wakes?

3. What are the economical implications of making layout changes in order to mitigate the impact of the wake effect?

1.3 Limitations

This work has been limited to a specific area in the SMB region with specific boundaries. The number of parameters considered in the sensitivity analyses was limited to keep the workload on a reasonable level.

The underlying wind data used for the calculations of wakes have been based on meteorological reanalysis data which should estimate the wind profile of the selected location. However, this data does not specifically reflect data gathered from the specific site and thus may not reflect specific site conditions.

The calculations made for the economic analysis are highly limited to available data based on estimation and extrapolation. This is due to the inability to access real economic data from active companies.

2. Theory

In the coming subchapters, the author intends to give a theoretical background to the work. Under section '2.1 Foundation' different turbine foundation types are covered. In '2.2 Wind Turbine Components' the different components of a wind turbine are explained. Further, under section '2.3 Wind in Different Forms' different wind conditions and variations are covered as well as what this means for a wind farm. Under section '2.4 Energy in the Wind' the author goes more into detail of how calculations on extractable energy from the wind are performed. Under section '2.5 The Wake Effect' different wake effect models are explained as well as the concept itself. Wind Shear models are covered in '2.6 Wind Shear' while '2.7 Site Assessment' covers different stages for the site assessment process. Lastly, a short description of LCOE is described under section '2.8 Levelized Cost of electricity'.

2.1 Foundation

The most common type of foundation is the monopile (Tong, 2010). It consists of a pile going through the seabed with a base (platform) over the sea water level, which the turbine tower is placed on. The part through which the power cable is directed to the seabed is called the J-tube. Foundation piles are usually made out of steel plates which are formed into cylindrical sections. The advantages of a monopile foundation is the relative simple production and installation as well as a possible application to a wide variety of depths. Monopiles are currently developed for increased water depth.

The tripod foundation consists of three legs which are going through the seabed (Tong, 2010). A foundation pile is then connected to the three legs, creating a base and a holder for the turbine tower. The base is more complicated as well as the installation process, which makes this foundation type more expensive. The benefits of this kind of base is mostly the stiffness that has its advantages in deeper waters but as the water depth increases, so does the base which can become quite large.

Jacket foundations increase in complexity as this foundation is made of relatively complex steel structure (Tong, 2010). The main advantage of this kind of foundation is a reduction in materials, and thus also a reduction in weight. Despite this advantage, jackets are relatively expensive. This foundation is mainly chosen for deeper water depths where the monopile foundation becomes unprofitable.

Gravity-based structure (GBS) uses the gravity in order to put the foundation in place (Tong, 2010). The foundation is usually made of concrete and the turbine tower is placed on the foundation. This foundation is mainly used for shallow waters but could be used in deeper waters as well. As the water depth increases, so does the need for larger bases in order to withstand the greater moments. The increase of the mass for the foundation depends on the water depth in a quadratic relation. A preparation of the seabed is needed in order to ensure a stable and horizontal floor and usually human divers are used in order to observe while the foundation is lowered to the seabed, making the process more dangerous.

As the water depth is increasing, the floating foundation gets more interesting (Tong, 2010). Floating structures are seen as the solution for installing wind towers on a water depth larger

than 70 meters. The floating structure needs to be attached to the seabed through securing cables.

2.2 Wind Turbine Components

The main components of a wind turbine are: the rotor, the drive train (generator, gearbox and brake), the yaw system (yaw drive and motor), the main frame (nacelle) and the tower (Manwell et al., 2009).

2.2.1 Rotor and Blades

The rotor consists of blades, hub and aerodynamic control surfaces (Manwell et al., 2009). The rotor is used in order to extract energy from the wind and convert it to rotational energy. Fatigue is a major concern as the rotor is exposed to varying loads. The varying loads in the rotor is also a reason why the drive train has to withstand a variety of loads.

The blades convert the force from the wind into torque that drives the rotational motion (Manwell et al., 2009). The blades should be constructed in order to be light in weight, but also strong in order to withstand the loads. The blades can either be fixed or variable where the angle against the wind is adjusted for maximum electricity production. This is achieved by obtaining a certain *tip speed ratio*, which is the quote between rotational speed and the speed of the wind. The optimal value of the *tip speed ratio* varies depending on how close the output is to the rated power.

2.2.2 Drive Train

The drive train includes the gearbox (if used), the generator, mechanical brake and shafts (Manwell et al., 2009). The shaft can either be directly connected (integrated) to the gearbox or seperated. The main reason behind different shaft couplings is because of the tradeoff between mechanical and electrical regulation control which can be done on different positions in the drive train depending on the manufacturer's design. In order to withstand the high stress, the main shaft is usually made out of steel.

2.2.3 Yaw System

Almost all wind turbines are equipped with a yaw system in order to align themselves in the wind direction (Manwell et al., 2009). The yawing is a slow process in order not to damage any important components. There are two different yaw systems; free yaw and driven yaw. The driven jaw system consists of a motor while free yaw systems rely on the aerodynamics of the rotor, and thus, most often are downwind turbines. The disadvantages of an active yaw system is the wear and tear moments caused by small movements of the turbine, causing damage to the teeth gear.

2.2.4 Main Frame and Nacelle

The main frame is used for mounting components and is usually made out of steel (Manwell et al., 2009). Here, components such as gearbox, generator, and brakes are mounted. Thus, these components can have a proper alignment between each other. The *nacelle* is the

whole ‘box’ on top of the tower, seen from the outside. It provides protection from weather and is made out of a light material.

2.2.5 Tower

The tower acts as a support in order to raise the main part of the turbine at higher heights (Manwell et al., 2009). Tower height is usually higher than 24 meters as the wind speeds are lower and more turbulent at lower levels. The most common material is steel or concrete. The tower must be dimensioned in order to withstand all the loads.

2.3 Wind in Different Forms

Globally, the wind conditions depend on differences in pressure over big geographical areas (Manwell et al., 2009). The differences in pressure occur because of an uneven distribution in the heating of the air from the sun. Generally the wind is heated around the equator and gets cooled at the poles. The rotation of earth around its own axis has further impact as the rotational speed around the equator is higher than the rotation speed close to the poles. In addition to this, local conditions can have an impact, such as the ground surface. Therefore, every site has different conditions for operating as a wind farm.

The wind varies on all time scales (Manwell et al., 2009). Inter-annually the variances in wind can be quite significant and have an impact on the long-term electricity production of the wind farm. Because of this, it can be as important to know the wind variations between the years as it is to know the variations during the year. Meteorologists claim that it takes 30 years of wind data at a certain location in order to know the long-term behaviour of the climate. However, it only takes 5 years of data in order to form an opinion of the average wind speed of the site. Data collections from shorter time periods can be useful. For instance, a rule of thumb that can be used is that 1 year of wind data can contribute to an evaluation of the average wind speed over the whole season with an accuracy of 10% and a confidence level of 90% (Aspliden et al., 1986).

The variations in wind during the year (on a monthly basis) depends on the location (Manwell et al., 2009). In Sweden, the electricity production from wind farms is higher during the winter months and lower production is achieved during the summer. Variations on an hourly basis are also occurring and most common is higher wind speeds during the day and a drop in wind speeds during the night. The hourly variations are caused by fluctuations in solar irradiation which are lowest during the winter months. Variations on a shorter time basis, such as less than 10 minutes, are considered to be turbulence.

Variations in wind can also occur in terms of direction. Seasonal variations are small, varying with a ~30° angle (Manwell et al., 2009). On a monthly basis the variations in wind direction can change up to 180°. However, when designing a wind farm, only the short-term variations in wind direction are important as the turbine needs to adjust to the dominating wind direction. This is regulated by the yaw control. Wind incoming with a wrong angle towards the blades has a negative impact on the lifetime of the blades and other mechanical parts of the turbine tower. A useful tool in order to analyze the wind data in accordance with direction is the wind rose diagram, seen in *figure 1*. It can be used to analyze the dominating wind direction for specific sites as it demonstrates the frequency of wind for different wind

directions. Specifically, this wind rose diagram is showing the frequency distribution of wind for the site used for the simulations. It can be seen that the dominating wind direction is from southwest, 255° from north in clockwise direction.

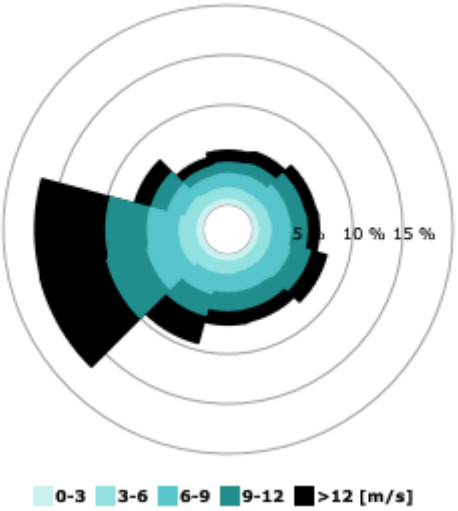

Figure 1. Wind rose diagram demonstrating the frequency of wind directions for the used site in the SMB region (NASA, 2019).

2.4 Energy in the Wind

Because the wind is the fuel for the wind farm, it is important to understand the possible extractable energy from the wind (EWEA, 2009). In that way, it can be known how much energy can be produced at the wind farm. The energy obtained from the wind is in kinetic form (Manwell et al., 2009). In order to decide the power output of the wind, the following formula can be used;

$$P(U) = \frac{1}{2}\rho A U^3 \quad (1)$$

Here, U is the wind speed, ρ is the density of air and A is the rotor plane area. Already here we can see that the available power is increasing with the cube of the wind speed. Therefore, a doubling of the wind speed gives eight times the wind power. Anyhow, this does not account for the losses in the drive train or the share of wind the rotor doesn't manage to capture (Manwell et al., 2009). If the rotor would capture 100% of the wind the rotor would be stationary as no wind would pass through. In order to obtain the electrical power produced by the wind turbine, the following formula can be used;

$$P_w(U) = \frac{1}{2}\rho A C_p \eta U^3 \quad (2)$$

Here, η is defined as the efficiency of the drive train (Manwell et al., 2009). On the other hand, C_p is the *power coefficient* which is defined as the share of possible wind power extracted by the rotor. The power coefficient can be obtained by the following formula;

$$C_p = \frac{Rotor\ power}{Power\ in\ the\ wind} = \frac{P_r}{\frac{1}{2}\rho A U^3} \quad (3)$$

The power coefficient can hold a value between 0 and 0.5926 where the maximal value is given by the *Betz limit* (Betz, 1919). Therefore, at most ~59% of the possible power in the wind will get captured by the rotor. In case the C_p value is 0 all wind passes through and no kinetic energy is converted into mechanical power.

2.5 The Wake Effect

As the wind turbine extracts energy from the wind, the downstream turbine will experience lower wind speeds (EWEA, 2009). This phenomenon is called the *wake effect*. Thus, one turbine can impact another turbine's performance. This can happen both within the wind farm (internal) or by one wind farm impacting another (external).

The wake effect is mainly placed in two different categories. The near wakes and the far wakes (Vermeer et al., 2003). The near wake is generally considered to be very close to the rotor, approximately one rotor diameter downstream. Therefore, the properties of the rotor such as number of blades and blade aerodynamics are of importance. However, the far wake goes beyond that and focus turns to the whole wind farm and interest turns to different wake models, wake interference, turbulence models and topographical effects. For estimation of the wake effects on a larger scale (on the level of a wind farm) the far wake models are more suitable.

2.5.1 The Jensen Model

One of the oldest and most accepted wake models is the Jensen wake model formulated in the early 1980s (Jensen, 1983). It is considered to be fairly simple, fast and easy to implement (Peña et al., 2015). It is used to calculate the reduction in wind speed downstream of a turbine. The reduction on wind speed is defined by the following equation;

$$\pi r_r^2 u_0 + \pi\left(r^2 - r_r^2\right) u_a = \pi r^2 u_1 \quad (4)$$

Where u_a is the ambient wind velocity, u_0 is the velocity just behind the rotor and u_1 is the velocity at a distance x from the rotor. The wake radius, r, can be expressed as;

$$r = ax + r_r \quad (5)$$

Where r_r is the radius of the rotor and a is the wake decay constant.

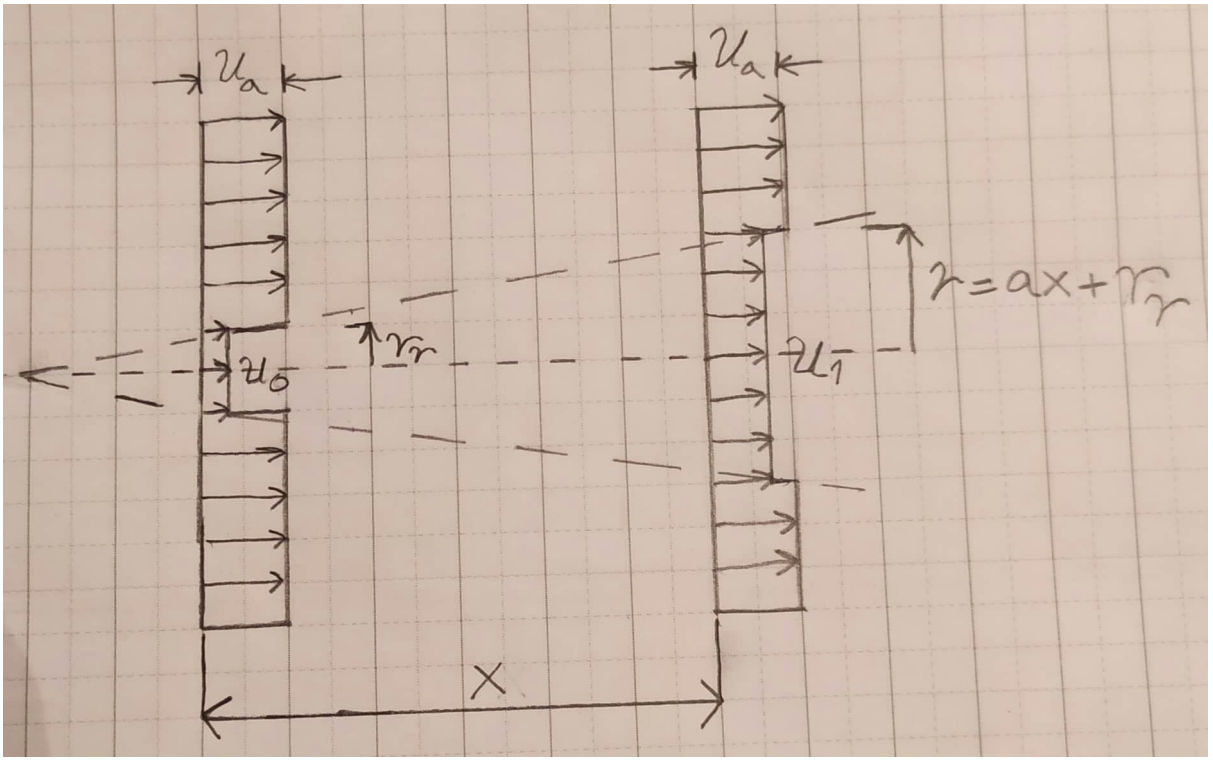

Figure 2. Schematic overview of the Jensen wake model (Jensen, 1983).

2.5.2 The Katić Model (Modified Park)

The Katić model (modified Park) was developed by using the Jensen model as a base (Peña et al., 2015). It is an empirical model based on linear expansion of the wake while considering balance of momentum (Beaucage et al., 2012). It was primarily developed for wind farm calculations in the Wind Atlas and Application Program (WAsP) software (Peña et al., 2015). The model is considered not so accurate under specific atmospheric inflow conditions as the results aren't identical with the meteorological data for a narrow range of wind speeds and directions. However, it is fairly accurate in predicting the wake losses on an annual basis. The following formula is used by the Katić model;

$$1 - \frac{u_2}{u_1} = \frac{1-\sqrt{1-C_T}}{\left(1+\frac{ax}{r_r}\right)^2} \qquad (6)$$

Where u_1 is the upstream wind velocity at the rotor, u_2 is the wind velocity at a distance x of the rotor, C_T is the thrust coefficient of the turbine, a is the wake decay constant and r_r is the radius of the rotor.

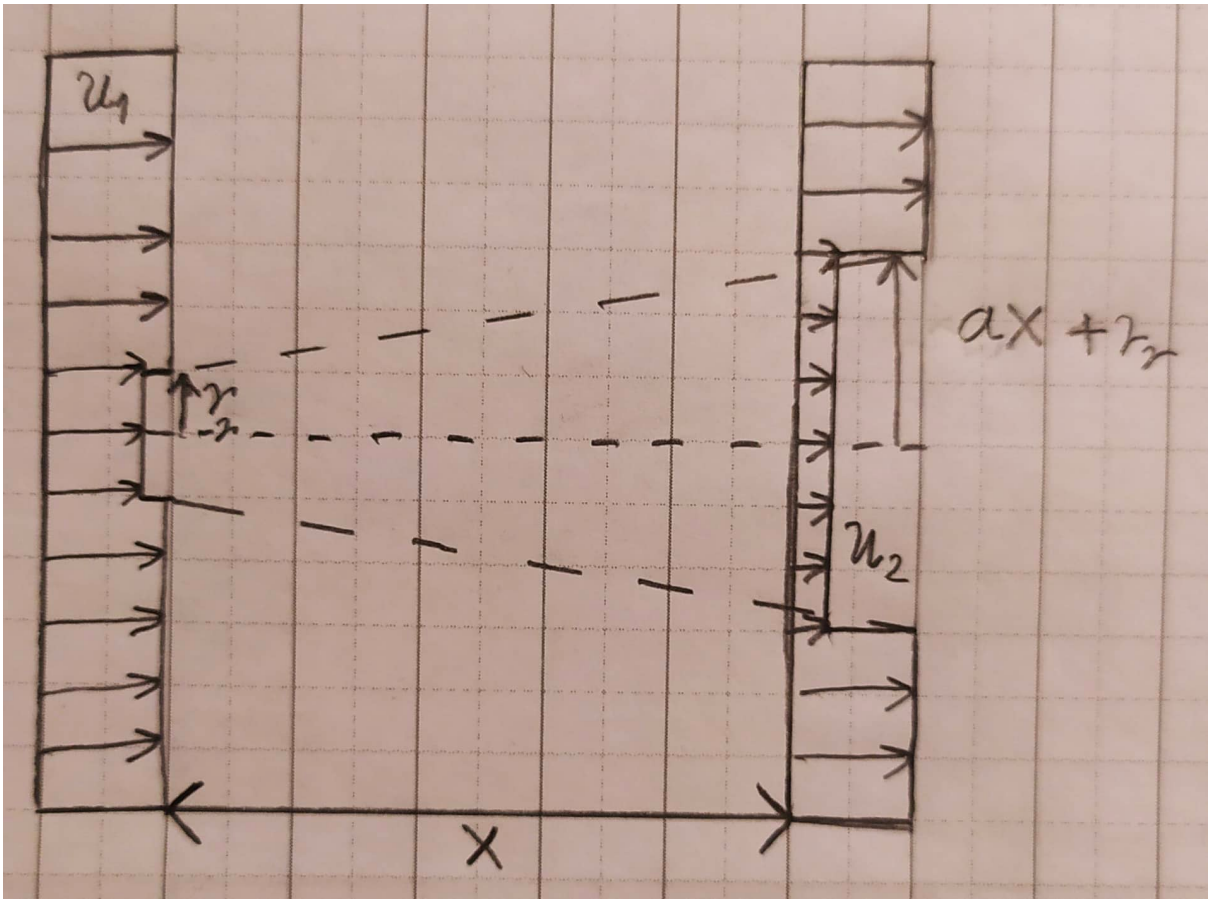

Figure 3. Schematic overview of the Katić wake model concept (Peña et al., 2015).

The biggest difference from the Jensen model is the consideration of the thrust coefficient, which is a way of describing the thrust force experienced by the turbine and the wake decay constant, which take into account the ambient turbulence intensity, turbine induced turbulence and atmospheric stability (Manwell et al., 2009). Therefore, it requires additional data of the environment and the turbine.

To conclude, the Katić model (modified Park) is an empirically derived equation based on the balancing of the momentum (Beaucage et al., 2012). The model assumes a velocity deficit occurring immediately after the turbine, which is derived from the specific turbine's thrust coefficient (C_T). In order to determine the wind speeds further down the stream, the wake decay constant (a) is used. Therefore, the wake downstreams is assumed to follow in a linear manner with the distance (x). In order to account for multiple wakes, superimposing or overlapping is used (Beaucage et al., 2012). Because of these simplifications, the model is considered to be rather fast and is desirable in software simulations where a fast approximation is more desirable than a precise answer.

2.5.3 The Eddy Viscosity Model

The Eddy Viscosity model is a more complicated model and based on the work of Ainslie (1988). The model solves RANS (Reynolds-averaged Navier-Stokes) equations in a cylindrical coordinate system with simplified assumptions (Beaucage et al., 2012). The model includes an eddy viscosity turbulence closure, therefore the name.

The ‘mixing in’ of the free stream wind around the wake is also considered at larger distances (Beaucage et al., 2012). This value is determined by the ambient turbulence intensity, as higher ambient turbulence intensity contributes to higher mixing rate and faster recovery of the wind. The Eddy Viscosity model was initially developed in order to be used together with the *WINDOPS* software, which is now called *WindFarmer*. The Eddy Viscosity model is a more complex model and therefore requires longer computational time. However, it contributes to more exact values of the wake effect calculation.

2.6 Wind Shear

Except from the wind conditions at the specific site, the surface of the site can also have an impact on the wind (Burton et al., 2001b). Furthermore, the velocity of wind varies for different heights above ground, which can be shown with wind shear models (vertical wind speed profile). A few relationships have been obtained for these purposes, both theoretically and empirically from a big range of observations. One alternative is the *Logarithmic Profile* or *Log Law*, where equation 7 is the mean wind speed (U_z) at height z meters above ground.

$$u_z = \frac{u_*}{k}\left[ln\left(\frac{z-d}{z_0}\right) + \Psi(z, z_0, L)\right] \quad (7)$$

Where U_* is the friction velocity, k is the Von Kármán constant, d is the zero plane displacement, z_0 is the surface roughness and Ψ is a stability term which can be neglected under neutral stability conditions. Typical values of z_0 are shown in table 1.

Table 1. Approximated values of surface roughness length for different types of terrains (Manwell et al., 2009).

Terrain description	z_0 **(mm)**
Very smooth (ice or mud)	0.01
Calm open sea	0.20
Blown sea	0.50
Snow surface	3.0
Lawn grass	8.00
Rough pasture	10.00
Fallow field	30.00
Crops	50.00
Few trees	100.00
Many trees, hedges, few buildings	250.00
Forest and woodlands	500.00
Suburbs	1500.00
Centers of cities with tall buildings	3000.00

Neglecting the stability term (Ψ) and the zero plane displacement (d) in formula (7), the following proportionality can be derived;

$$u_z \propto ln\left(\frac{z}{z_0}\right) \quad (8)$$

Which can further be simplified into the following approximation;

$$u_z \propto z^a \quad (9)$$

The approximation in formula (9) is usually called the *Power Law Profile*, where the value of exponent a is typically equal to 1/7 (Burton et al., 2001b). However, in practice, the value of a varies over different height intervals.

2.7 Site Assessment

The main aim of a correct site assessment is to maximize electricity production and to minimise capital and operating cost (EWEA, 2009). Therefore, it could be claimed that the real purpose of the site assessment is to deal with uncertainties and minimize risks.

2.7.1 Micro-siting

When the constraints of the wind farm are clearly defined, a process for optimization of the layout is initialized (EWEA, 2009). This process is called *Micro-siting* with the aim to minimize the cost of infrastructure. At the same time, turbines are placed in such a way to maximize the total production. Generally, it is considered that the profitability of the project is more dependent on energy production than infrastructure cost and thus, energy production is prioritized during the layout design. However, infrastructure and operating costs can make a project unprofitable.

A detailed design is often created by a wind farm design tool (EWEA, 2009). This is used in order to make a model of the layout, predict the electricity production and in some cases, address issues of noise or visuals. Even small gains achieved in the electricity production due to layout modelling can have an immense impact, as these gains are accomplished with almost no increase in capital costs.

2.7.2 Visual Influence and Noise

Visual impacts from a wind farm is an usual issue for many wind farm projects, especially for projects that are planned in population dense areas (EWEA, 2009). A few design tools are available for assessing the visual influence from different angles. For offshore wind farms with long distances from the shore, the visual influence is usually not a problem.

Noise can also be a problem for the local residents and in such cases, noise can be a limiting factor for maximum electricity production (EWEA, 2009). Blades, gearbox and generator is elevated and free from obstacles, making the propagation of sound easy. In rural areas, where the background noise is very low, this can have a bigger impact. In fact, the biggest impact usually occurs during low wind speeds, as the background noise tends to

be low during these moments. Noise is very rarely a problem for wind farms located offshore.

2.7.3 Turbines

In order to effectively use the chosen area for the project, a minimum spacing between turbines is desirable (EWEA, 2009). The optimal spacing between turbines is heavily dependent on the specific terrain and the dominating wind direction. For a spacing less than five rotor diameters, unacceptably high wake losses will occur. Too narrow spacing will also result in more turbulence due to wake from upstream turbines, leaving heavier mechanical loads on the turbines. Generally, wider spacing in the dominating wind direction is beneficial.

2.7.5 Cables

Cables are constructed to handle all three phases and an additional optical fibre cable for communication (EWEA, 2009). Additional fillers and protective layers are added in order to prevent any water leakage. Cables laid internally in the wind farm (intra-array) are rated at 30 kV to 36 kV. A few turbines are connected to the same cable, forming different lines (or sectors) gathering at the substation. Each 'line' is usually not rated higher than 30 MW. The exporting cable (leaving the substation) are of similar design but must support higher voltages than the individual sector lines. These cables are normally rated at around 100kV to 220 kV.

At the wind turbine, cables are passing vertical tubes from the seabed called the J-tube or I-tube in order to reach the switchgear (EWEA, 2009). They are buried under the seabed in order to ensure reliability and prevent damages from trawlers and anchors, and the exposure to hydrodynamic loading. Because of the vertical cable tube there is additional cable length needed than simply the measured distance between the two turbines. Therefore, the length of the cable tube needs to be considered, which in turn impacts the total cable length required and the capital costs of the project.

2.8 Levelized Cost of Electricity

Levelized cost of electricity (LCOE) is an approach to estimate the discounted costs over a lifetime for the ownership and generation of the asset (Aldersey-Williams & Rubert, 2019). The LCOE is given by the following formula;

$$LCOE = \frac{sum\ of\ costs\ over\ lifetime}{sum\ of\ electricity\ produced\ over\ lifetime} = \frac{\sum_{t=1}^{n} \frac{I_t + M_t + F_t}{(1+r)^t}}{\sum_{t=1}^{n} \frac{E_t}{(1+r)^t}} \quad (10)$$

Where I_t is the investment expenditures (at year t), M_t is the operations and maintenance expenditures (at year t), F_t is the fuel expenditures (at year t), E_t is the electricity generation

(at year t), *r* is the discount rate and *n* is the economic lifetime of the system. Note that the fuel expenditures are set to zero for wind power, as the fuel is the wind.

3. Method

In the coming subchapters, the author explains the methodology used in order to achieve the aim of this work. The chapter is divided in 3 subchapters where '3.1 Future Trend Predictions' covers the predictions that were made for the rotor diameter, turbine height and hub height. In section '3.2 WindFarmer' the methodology for the simulations made in this work is explained. Lastly, under section '3.3 Economic Analysis' the methodology of economic analysis is explained.

3.1 Future Trend Predictions

In order to make the results of this study more aligned with future trends the author has attempted to predict the development of wind turbine characteristics using past available data. In this way, the results can be put into context for today's offshore wind farm development as well as future implications. For this purpose, there is a need to decide what is a reasonable rated power for the future offshore wind turbines being investigated. Based on the rated power, the rotor diameter and the turbine height will be derived.

According to IRENA (2019) offshore wind turbines are expected to reach a rated power of 15 - 20 MW in the years between 2025 and 2030. Considering this information, two representative offshore wind turbines were chosen as plausible, one of 16 MW rated power as well as one of 17 MW.

3.1.1 Rotor Diameter

In order to predict the future rotor diameter linear regression was used. Here, a dataset of past rotor diameter trends adjusted to installed turbine power were used in order to obtain a linear regression curve. The used dataset can be seen in Appendix 1.

The trend of the dataset appeared to evolve in a linear fashion and therefore linear regression was considered a plausible approach. However, this dataset does not include data of a turbine that exists today. Therefore, this dataset was supplemented with the most powerful offshore wind power turbine currently in operation, namely Haliade-X 12 MW turbine from General Electric (GE Renewable Energy, n.d.). This turbine has a rotor diameter of 220 meters.

Using linear regression, the rotor diameters for two future turbines were predicted using a rated power of 16 MW and 17 MW. The obtained linear regression model had a m-value of 12.5779 (error ± 1.77185) and a c-value of 47.4062 (error ± 11.9647). Using this model the predicted rotor diameter for 16 MW and 17 MW was 248.65 m and 261.23 m respectively. The obtained linear regression curve can be seen in figure 4.

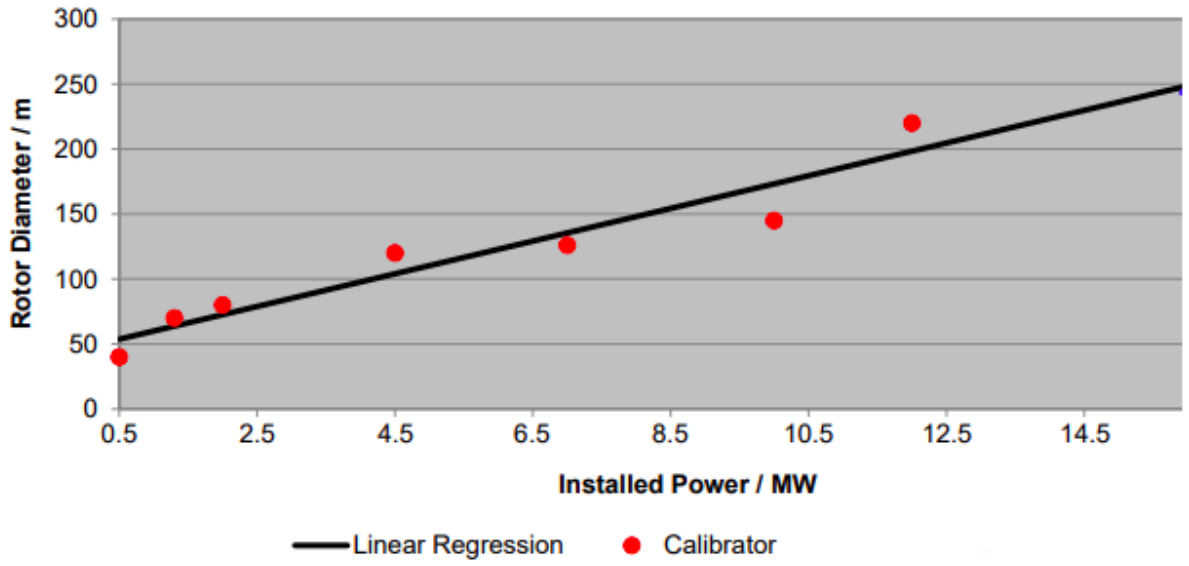

Figure 4. Obtained linear regression curve from historical data points of rotor diameter as a function of installed turbine power.

3.1.2 Turbine Height

The dataset used for the future predictions of turbine heights was adjusted to the rated power. This dataset originally included a prediction of the turbine height for a 12 MW turbine. However, this data point was replaced by the 12 MW Haliade-X turbine from General Electric as the data obtained from a turbine currently in operation is considered more accurate than a prediction (GE Renewable Energy, n.d.). According to GE, the height of this turbine is 260 meters. The dataset used for this purpose can be seen in Appendix 2.

For the prediction of future turbine height another regression mode was used. Here, the given dataset was considered to behave in a nonlinear fashion and four parameter logistic (4PL) regression was considered the best applicable model to the existing dataset. The prediction of future turbine heights was made for two turbines with a rated power of 16 MW and 17 MW.

The four parameter logistic (4PL) regression model obtained an a-value of -15.687, b-value of 0.516861, c-value of 6 683 907 116 and a d-value of 8 982 749. Using this regression model the predicted turbine height for the 16 MW and 17 MW turbines was 298.79 m and 308.80 m respectively. The obtained regression curve can be seen in figure 5.

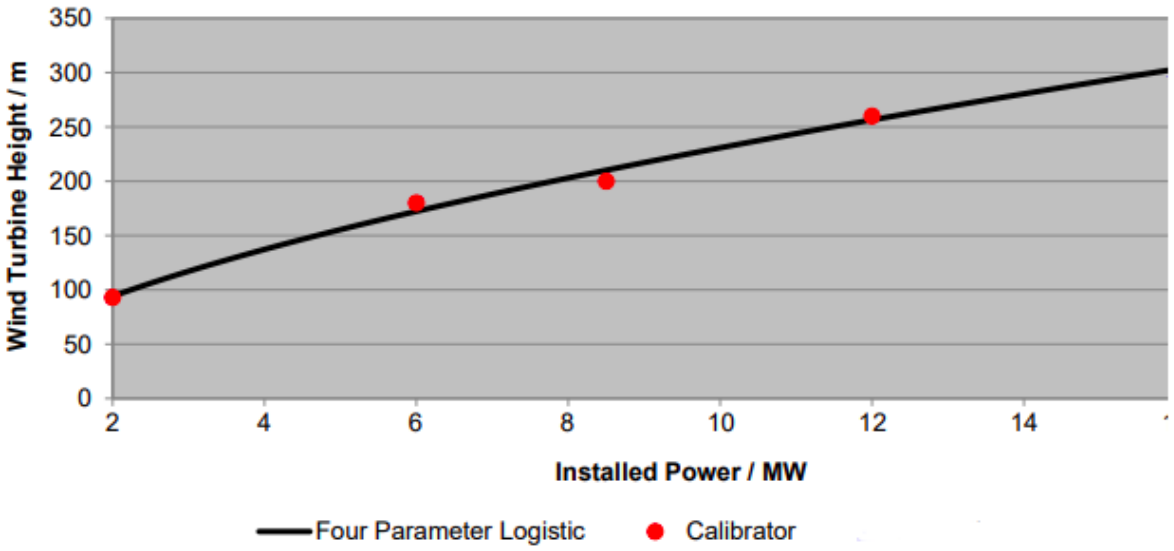

Figure 5. The obtained four parameter logistic regression curve from historical data points of wind turbine height as a function of installed turbine power.

3.1.3 Hub Height

The hub height is considered to be the turbine height minus half of the rotor diameter (or the radius of the rotor). Thus, the hub height for the 16 MW and 17 MW turbine can be calculated by the results obtained from the regression models of rotor diameter and turbine height. For the 12 MW turbine the calculation was based on the data given by GE. The hub height for the 12 MW was 150 m while the predicted values for the 16 MW and 17 MW turbine was 174.5 m and 178.2 m respectively.

3.2 WindFarmer

For the simulations the software program *WindFarmer: Analyst* v. 1.2.2 by DNV GL was used.

3.2.1 Project Location

A specific project location and area need to be chosen in the software program *WindFarmer: Analyst.* This has been done by using coordinates. The specific site location was set to 55,529274 17,134978 (Latitude, longitude). However, the specified area was inspired by an application to the *Finnish Ministry of the Environment*, from the company *Baltex Power S.A* (2011). The specific WGS84 coordinates are given in Appendix 3.

As *WindFarmer: Analyst* does not support the WGS84 coordinate system, the coordinates needed to be converted into the UTM coordinate system. Thereafter the coordinates were applied to the map as accurately as possible. The exact coordinates used for the project area are given in Appendix 4. The resulting boundary area used in *WindFarmer: Analyst* can be seen in figure 6.

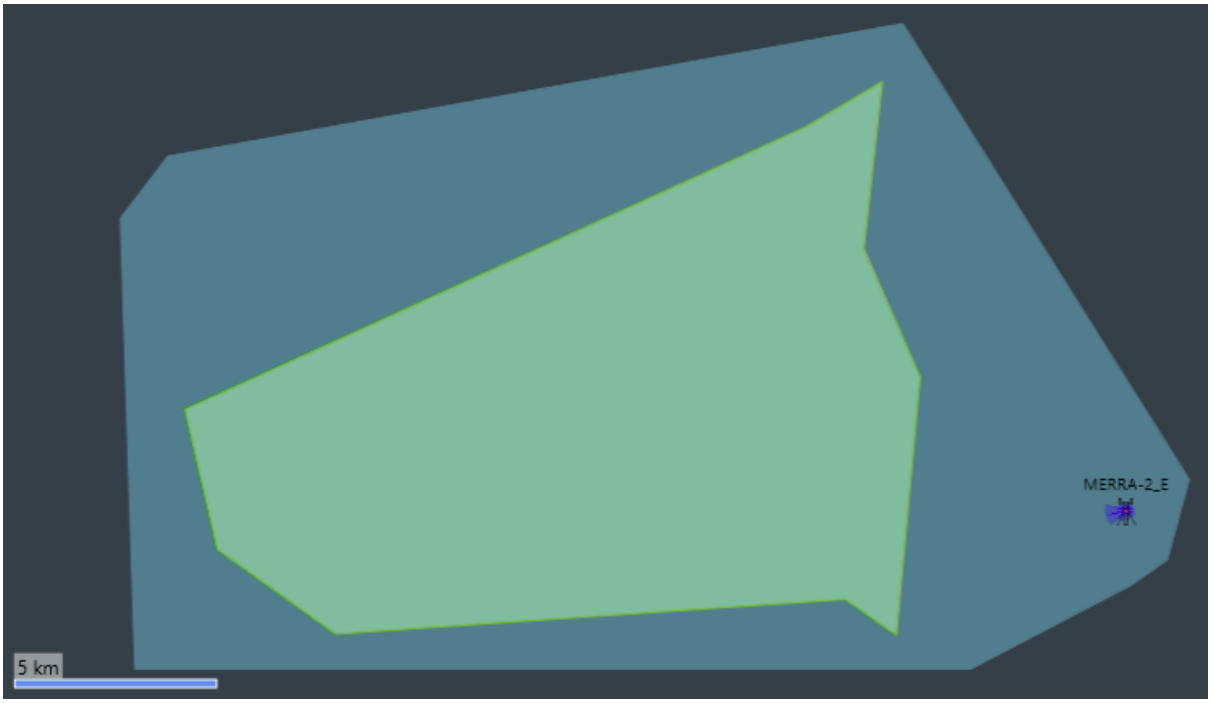

Figure 6. Wind farm boundary area in green obtained from the UTM coordinates.

3.2.2 Wind Data

Wind data was given by the *Reanalysis data* service in *WindFarmer: Analyst* which inputs the wind data from the MERRA-2 database for a certain location (NASA, 2019). The exact coordinates for the location used was 657908,57773 mE (Latitude) and 6153273,1002 mN (Longitude). The name of this mast set for this location was named *MERRA-2_E* as can be seen in figure 6 (NASA, 2019). The wind speed and the wind direction data was obtained at a height of 50 m above the ground level.

3.2.2.1 Wind Shear Model

Using the MERRA-2_E measurement calculations, different shear model setups were used. For instance, when the logarithmic profile was used, the site roughness (Z_0) was set to 0.00055 m, suitable for blown sea terrain (Manwell et al., 2009). At other times, when the power law was used, the power coefficient (α) was set to 0.11 in order to reflect the condition at sea under near-neutral stability conditions (Hsu, Meindl & Gilhousen, 1994). The reason for using two different shear models is the fact that some calculations in *WindFarmer: Analyst*, such as wake calculation based on modified Park, derive wakes from site roughness.

For the site roughness (Z_0) a further sensitivity analysis was done with two additional values. The lower value was set to 0.00020, representing calm sea terrain while the higher value was set to 0.0010 m in order to simulate the presence of waves (Manwell et al., 2009). The sensitivity analysis was performed on the base case layout of a 16 MW turbine with 7D distancing (see section 3.2.5) for both Eddy Viscosity and Modified Park wake model.

3.2.3 Turbine Types

In total 3 different standardized wind turbine profiles were used, Generic Turbine 12.0 MW Extrapolated, Generic Turbine 16.0 MW Extrapolated and Generic Turbine 17.0 MW Extrapolated. As the name suggests, the power curve was derived by extrapolation of the Generic Turbine 3.0 MW profile provided by the *WindFarmer: Analyst* demo data. This was done by increasing the power output with the same factor at all wind speeds in order for the power curve to reach its new maximum power output at the same wind speeds as for the initial turbine. However, the hub height and the rotor diameter were derived from the different regression models named under section *3.1 Future Trends and Predictions* while the thrust curve was kept the same as for the given 3.0 MW turbine. Specifications for each turbine can be seen in Appendices 5 - 8.

3.2.4 Flow Model

The flow model setup was specified by the flow field boundary seen in Appendix 9 where the target height was adjusted to the hub height of the respective turbine. The simplified model was used, meaning that wind data from the MERRA-2 database was used and extrapolated with help of the shear model in order to reflect the wind circumstances at the hub height (NASA, 2019). In this way, a flow model was obtained.

3.2.5 Turbine Layout and Simulations

Each turbine has specific coordinates for each layout. The separation distance (spacing) between turbines is given in terms of number of turbine diameters. The number of turbines, rated power and distancing is varied for each layout, but the base case set up is considered to be the 16 MW turbine with a distancing of 7 rotor diameters (circular separation). Based on the base case setup one parameter is changed at a time in order to interpret the impact.

3.2.5.1 Partial Wind Farm Case

The partial wind farm case set up consists of 20 turbines (5x4) symmetrically placed in the wind farm boundary area. The circular spacing between turbines could hold three different values; 4 rotor diameters (4D), 7 rotor diameters (7D) and 10 rotor diameters (10D) for the 16 MW turbine. However, elliptical distances were also used where the distance was either 7D x 4D or 10D x 7D with the direction of 255° from north, defined by the long axis. This value was chosen based on the dominating wind direction which can be seen in figure 1. The rated power is varied as well but the 7 rotor diameter spacing was kept constant. The rated power could hold three different values; 12 MW, 16 MW and 17 MW. In total, 7 different layouts were simulated for the partial wind farm case scenario, which can be seen in table 2.

Table 2. Demonstration of all layouts simulated for the partial wind farm case. Gray area indicates the layout combination has not been simulated.

Separation Distance \ Rated Power	12 MW	16 MW	17 MW
Circular distance 4D			
Elliptical distance 7Dx4D			
Circular distance 7D			
Elliptical distance 10Dx7D			
Circular distance 10D			

The partial wind farm case scenario of 20 turbines (5x4) for the base case representing 16 MW turbines with 7D distance can be seen in figure 7, where the smaller blue circles represent the turbine, the bigger white circles represent the separation distance. An increase of the rated power follows that the separation distance increases as well due to larger rotor diameter. The opposite is true for a decrease of the rated power.

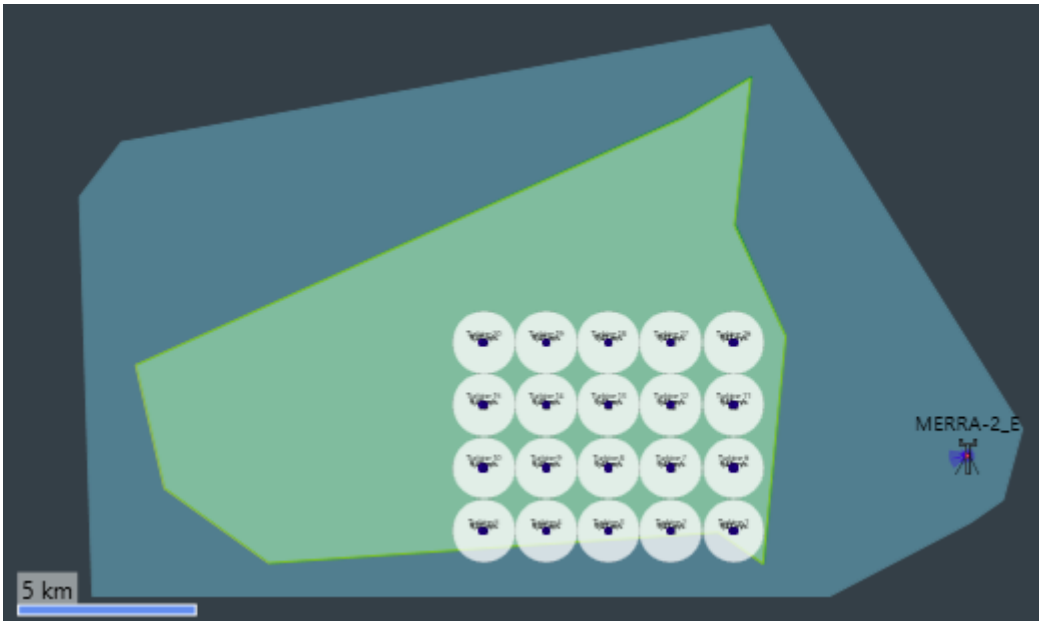

Figure 7. Base case of the partial wind farm case scenario with 20 turbines (5x4). The layout consists of 16 MW turbines with 7D spacing.

Every different layout will imply that the turbines need to be moved in order to comply with the new constraints. In figure 8, the layout of the same 16 MW turbine can be seen, but now with elliptical separation distancing of 10D x 7D. The change in the distancing constraint forces the turbines to be moved, taking up a larger area. However, the layout was kept symmetrical and fitted to the lower right corner of the boundary area in order to seek consistency.

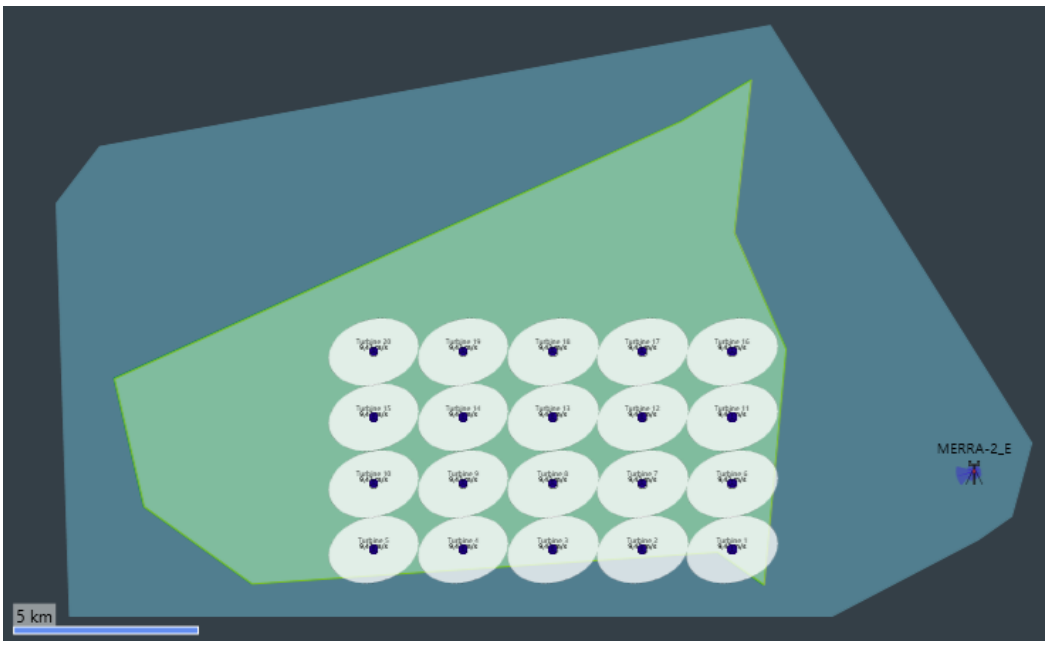

Figure 8. Partial wind farm case scenario with 20 turbines (5x4). The layout consists of 16 MW turbines with 10D x 7D elliptical spacing.

Common for all partial wind farm case layouts is the placing of turbine 1, which is placed in the bottom right corner with x-coordinate 651391 (UTM coordinate system) and y-coordinate 6151159. All other turbines are placed symmetrically according to the spacing requirements.

3.2.5.1.1 Rotor Diameter Sensitivity Analysis

The rotor diameter sensitivity analysis was carried out using the partial wind farm case set up (5x4 turbines). However, only the base case layout (16 MW with 7D spacing) was used. In the rotor diameter sensitivity analysis, the rotor diameter is decreased by 20%, as well as increased by 20% in order to interpret the impact of the rotor diameter.

3.2.5.1.2 Hub Height Sensitivity Analysis

A hub height sensitivity analysis was performed as well on the same partial wind farm case set up (5x4 turbines) with the base case layout (16 MW with 7D spacing). Here, the impact of hub height was evaluated for 4 different values; decreased with 20%, decreased with 10%, increased with 10% and increased with 20%.

3.2.5.1.3 Electricity Production per Square Meter

Most of the simulations are based on the change of parameters that have an impact on how well the defined area is used. For instance, bigger turbine spacing gives the opportunity for the wind speeds to recover to a higher degree. However, such a change will imply that the area is less utilized. Therefore, an analysis of the electricity production per square meter is done by dividing the electricity yield (considering wake effects) with the area. The area is considered the field that the turbines cover including the turbine foundation and swept area. However, the separation distance required for the turbines along the edges of this field is not included in the definition of the area.

3.2.5.1.4 External Wake from a Neighbouring Cluster

An identical cluster, with the same dimensions as for the base case setup, was placed to the left of the existing base case setup. For maximum wake impact, the second cluster should be placed in the dominating wind direction (255° from north). However, for simplicity, the second cluster was placed immediately to the left (270° from north). Here, the distance *L* (8 715 m) is the horizontal length of the base case setup, considered to include the 5 turbines along the horizontal axis together with the distancing constraints. Therefore, the distance *L* is the same as 35 rotor diameters (7 rotor diameters for each turbine). The impact of external wakes from the added cluster to the left were simulated for 5 different lengths; 2*L* (17 430 m), 1*L* (8 715 m), ½*L* (4 357.5 m), ¼*L* (2 178.8 m) and ⅛*L* (544.7 m). The length was measured as the distance to the closest turbine in the horizontal direction (including the distance constraint of the turbine). The layout used is the base case layout with 16 MW turbines and 7D spacing. An illustration of the length of the cluster can be seen in figure 9. The distance between the two clusters is ½L.

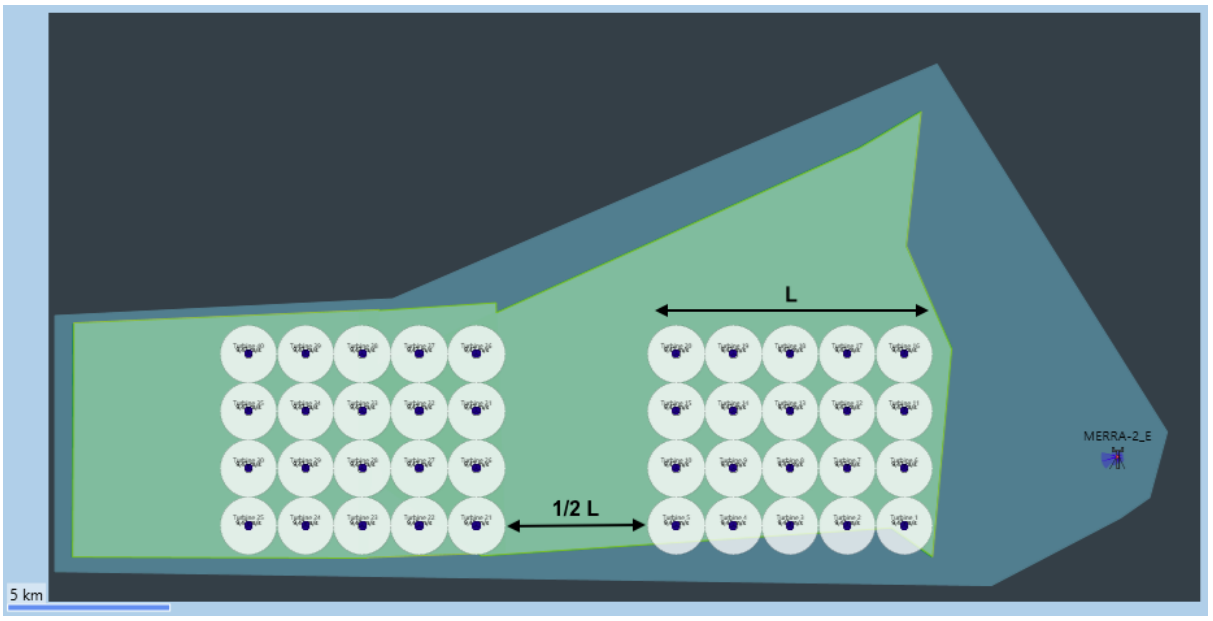

Figure 9. Illustration of the length of the cluster and the distance between two clusters.

3.2.5.2 Wind Farm Case

The wind farm case is based on the idea of filling the whole wind farm boundary area with the maximal number of turbines in order to simulate a scenario of a potential wind farm. Therefore, the number of turbines fitted will depend on the rotor diameter as well as the separation distance. The same number of layouts were simulated as for the partial wind farm case scenario, demonstrated in table 2. The layout for the 16 MW turbine with 7D circular spacing can be seen in figure 10.

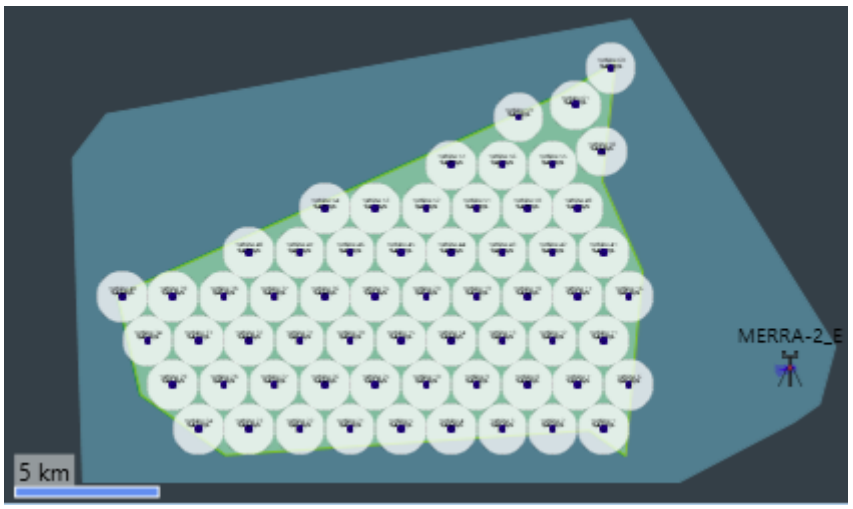

Figure 10. Wind farm case. The layout consists of 16 MW turbines with 7D circular spacing.

The layouts for the wind farm case are based on the position of turbine 1 in the bottom right corner, where the rest of the turbine placements are placed symmetrically according to the spacing requirements. In figure 11, it is illustrated how the layout changes when the spacing requirements change.

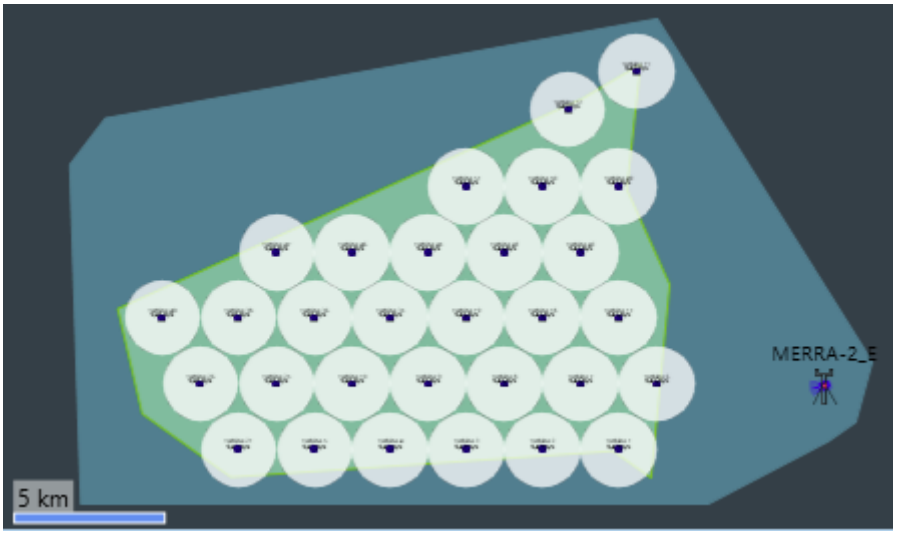

Figure 11. Wind farm case. The layout consists of 16 MW turbines with 10D circular spacing.

The position of turbine 1 for all the layouts based on the wind farm case can be seen in Appendix 10. For every layout, some of the turbines deviate from the symmetrical placings in order to utilize the area as much as possible and are given in Appendix 11 - 17. The same layouts were simulated for wake calculation as for the partial wind farm case, given in table 2. In addition to the wake calculation, the wind farm setup was used in order to perform the sector management analysis, seen under section *3.2.5.2.1 Sector Management* as well as the economic analysis, which can be found under section *3.3 Economic analysis.*

3.2.5.2.1 Sector Management

Sector management was performed in order to evaluate the impact on electricity production when different sections are limited for a certain range of wind speeds. It was performed on the wind farm layout with 7D distancing and 16 MW turbines. The layout consists of 61 turbines and was divided into 3 groups; The 20 best performing turbines (green), the 20 worst performing turbines (red) and 21 turbines in between (yellow) as can be seen in figure 12. The sector management was performed for the wind speed ranges of 2-7 m/s, 20-25 m/s and 23-25 m/s. The turbines actually used in the sector management simulation were the 20 best performing, as well as the first 5 downstream turbines among the worst performing, marked with gray shadows in figure 12.

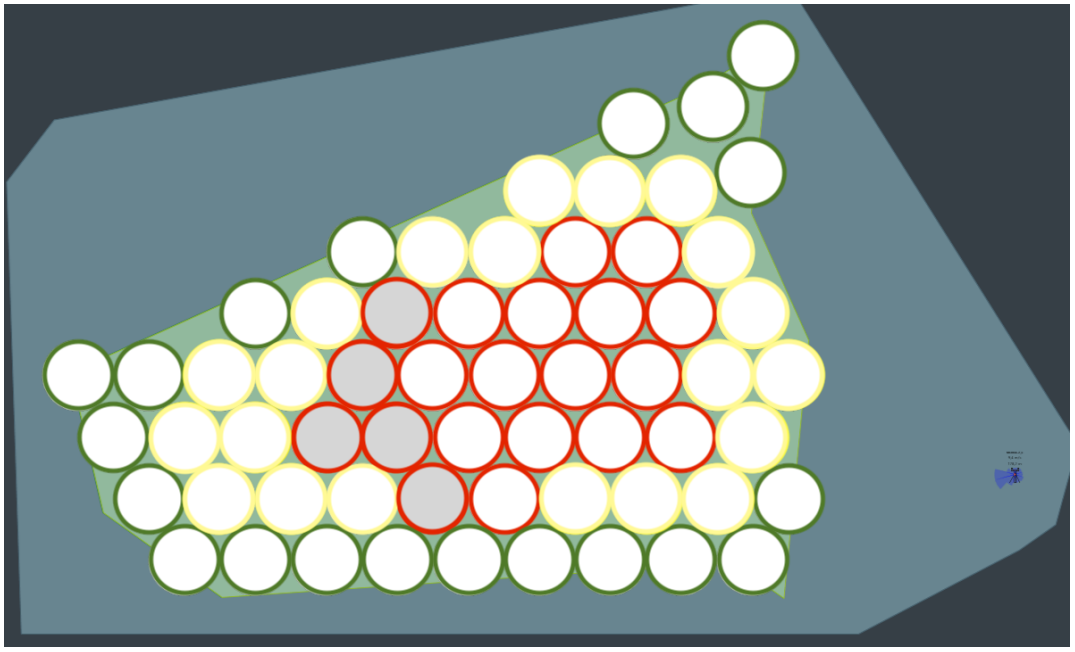

Figure 12. Layout of 16 MW turbines with 7D spacing marked with colors according to their performance (wind farm case).

3.2.6 Wake Calculation

The wake calculation was done using *WindFarmer: Analyst* by either using the Eddy Viscosity model (10% turbulence intensity) or the Modified Park model based on the site roughness (see section 3.2.2.1).

3.3 Economic Analysis

In order to find out the economical impact of the different measures an economic analysis was done for three layouts of the wind farm case. Namely, layout with 7D distancing, layout with 10D x 7D elliptical distancing and the layout with 10D distancing. All layouts were based on the 16 MW turbine.

3.3.1 Foundation and Turbines

Due to a relatively small sea depth of 25-35 m, a gravity base foundation was proposed for the used site (Baltex Power S.A., 2011). The foundation costs were estimated to be 400 000

€ / m for the first 10 meters with a price increase of 5% (420 000 € / m) for depths over 10 meters (Svensson, 2019). Due to unknown variability of the water depth at the site location, an average depth of 30 m was chosen. As the foundation never changes between layouts, the foundation cost was 12 400 000 € each.

The cost of turbines was also based on the course material by Svensson (2019) where the cost was estimated to be 1 400 000 € / MW for turbines rated under 3 MW. For larger turbines, the cost decreased with 2% for every MW added thereafter. Thus, the cost decreased exponentially when passing a rated power of 3 MW.

3.3.2 Cable Layout and Transformers

A cable layout was suggested based on the rule of having maximum 7 turbines for each single cable line. This is done in order to keep the cable dimensions low. Two cable dimensions were used based on the course material from Svensson (2019). The lower dimensioned cable used was 185 mm^2 supporting up to 21 MW and thus only one turbine. The thicker cable used was 400 mm^2 supporting up to 117 MW and thus also supporting a single cable line of 7 turbines. The complete cable layouts used together with transformers can be seen in Appendix 18 - 20. The estimated cost for the 185 mm^2 cable is 450 000 € / km including installation costs while the 400 mm^2 cable had an estimated cost of 750 000 € / km.

The cable length was estimated both under water (on seabed) and at the turbine site. In order to estimate the length needed between turbines, simply the distance was measured in *WindFarmer: Analyst*. However, for the estimation of cable length at turbine site, a depth of 30 m was used based on the estimated 25 - 35 m depth for the area (Baltex Power S.A., 2011). Another 10 m was added due to the platform height above sea level as well as additionally 5 m loose cable on both ends. In total, 50 m was estimated needed for the j-tube and the platform. The total cable length needed for each layout (both on the seabed and at the turbine site) can be seen in table 3.

Table 3. Cable length needed for each wind farm layout. The length is divided by the length needed on the seabed as well as the cable length needed at the turbine site.

Wind Farm Layout	**185 mm^2**	**400 mm^2**
16 MW Circular distance 7D		
- On the seabed	37 140.1 m	72 005.5 m
- At turbine site	2 100 m	4 000 m
16 MW Elliptical distance 10Dx7D		
- On the seabed	39 848.2 m	45 503.9 m
- At turbine site	1 800 m	2 400 m
16 MW Circular distance 10D		
- On the seabed	43 081.4 m	31 246.4 m
- At turbine site	1 700 m	1 300 m

All three layouts were constructed with 2 different transformers which cables are connected to. They are placed in near proximity in order to have a mutual connection point to the

exporting cable, which is not included in the cable layout. The transformer capacity for each wind farm layout can be seen in table 4.

Table 4. Description of transformer capacity needed for different wind farm layouts.

Wind Farm Layout	Transformer 1	Transformer 2
16 MW Circular distance 7D	432 MW	544 MW
16 MW Elliptical distance 10Dx7D	336 MW	336 MW
16 MW Circular distance 10D	208 MW	272 MW

The transformer costs were based on the course material by Svensson (2019) and estimated to be 180 000 € per MW for capacity needed under 360 MW. For installed capacity between 360 - 500 MW, the cost was estimated to be 170 000 € per MW. For capacity over 500 MW, the cost was estimated to be 160 000 € per MW.

3.3.3 Levelized Cost of Electricity

The levelized cost of Electricity (LCOE) was calculated for the different layouts in order to estimate the cost of produced electricity and therefore, show the impact on the electricity cost based on the different layouts. In order to estimate the cost of produced electricity, the total cost needed to be taken into account which can be seen in table 5. The total cost was considered to be the capital cost.

Table 5. Costs of the different investments with a summation of total costs for each layout.

Investment Type	Cost
16 MW Circular distance 7D	
- Turbines	1 165 638 575 €
- Foundation	756 400 000 €
- Transformer stations	172 680 000 €
- Cables	74 662 170 €
Total	**2 169 380 745 €**
16 MW Elliptical distance 10Dx7D	
- Turbines	802 570 822 €
- Foundation	520 800 000 €
- Transformer stations	120 960 000 €
- Cables	54 669 615 €
Total	**1 499 000 440 €**
16 MW Circular distance 10D	
- Turbines	573 264 873 €
- Foundation	372 000 000 €
- Transformer stations	86 400 000 €
- Cables	44 561 430 €
Total	**1 076 226 300 €**

The annual operation & maintenance costs were assumed to be 1.6% of the capital cost, according to the course material from Svensson (2019). No insurance or balancing costs were added. Total lifetime of the project was assumed to be 25 years, together with a discount rate of 7%.

3.3.3.1 Increased Hub Height

An analysis of the impact of increased hub height was performed in order to see if the additional electricity yield overweights the investment cost. The evaluation of increased electricity production was done with the *WindFarmer: Analyst* software where the logarithmic profile was used, described under section *3.2.2.1 Wind Shear Model*. The impact of increased hub height was performed for 3 heights; 184.5 m (10 m increase), 194.5 m (20 m increase) and 204.5 m (30 m increase).

4. Results

This chapter is divided into two subchapters, where the results from the simulations are presented under '4.1 Simulations' and the results from the economic analysis are presented under '4.2 Economic Analysis'.

The subchapter covering simulations is proportionally longer, divided into subsections; shear model, wake model, wind farm case, electricity production per area, rotor diameter sensitivity analysis, hub height sensitivity analysis, site roughness sensitivity analysis, sector management and external wake from neighbouring cluster.

4.1 Simulations

The results from the wake calculation are presented as lost electricity production due to wakes. All simulations are based on the partial wind farm case, except for the results under section *4.1.3 Wind Farm Case, 4.1.8 Sector Management* and *4.2 Economic Analysis*, which are based on the wind farm case.

4.1.1 Shear Model

4.1.1.1 Log Profile

The lost electricity production due to wakes, using the logarithmic profile (Z_0 = 0.00055 m), is given in table 6. Here, the Eddy viscosity wake model was used. It can be seen that the impact of wakes increases with narrow spacing. The impact of both a decrease and increase in rated power seem to enlarge the impact of wakes, but the result is not entirely clear as the differences are small.

Table 6. Loss of electricity production due to wakes for the partial wind farm case using logarithmic profile (Z_0 = 0.00055 m) and Eddy viscosity wake model.

Separation Distance \ Rated Power	12 MW	16 MW	17 MW
Circular distance 4D		~10.7%	
Elliptical distance 7Dx4D		~7.1%	
Circular distance 7D	~4.9%	~4.8%	~4.9%
Elliptical distance 10Dx7D		~3.7%	
Circular distance 10D		~2.9%	

4.1.1.2 Power Law

The lost electricity production due to wakes, using the power law wind profile (α = 0.11) is given in table 7. The wake calculations are based on the Eddy viscosity wake model. The results are very similar to the results in table 6 using the logarithmic profile, suggesting that the parameters used in both models give fairly equivalent results. However, the power law wind profile (using a 0.11 power exponent) gives somewhat lower values, especially for the narrower spacing constraints.

Table 7. Loss of electricity production due to wakes for the partial wind farm case using the power law profile (α = 0.11) and Eddy viscosity wake model.

Separation Distance \ Rated Power	12 MW	16 MW	17 MW
Circular distance 4D		~10.1%	
Elliptical distance 7Dx4D		~6.7%	
Circular distance 7D	~4.6%	~4.5%	~4.6%
Elliptical distance 10Dx7D		~3.5%	
Circular distance 10D		~2.7%	

4.1.2 Wake Model

The lost electricity production due to wakes, using the modified Park wake model can be seen in table 8. The calculations are based on the logarithmic profile with the same roughness as in table 6, making the tables comparable. The results follow the same pattern of higher impact of wakes for narrower spacing. However, using the modified Park model results in higher calculated impact of wakes for all layouts. Here too, it is not clear how a change of rated power impacts the wakes.

Table 8. Loss of electricity production due to wakes for the partial wind farm case using logarithmic profile (Z_0 = 0.00055 m) and modified Park wake model.

Separation Distance \ Rated Power	12 MW	16 MW	17 MW
Circular distance 4D		~14.1%	
Elliptical distance 7Dx4D		~9.8%	
Circular distance 7D	~7.0%	~6.9%	~6.9%
Elliptical distance 10Dx7D		~5.3%	
Circular distance 10D		~4.1%	

4.1.3 Wind Farm Case

The lost electricity production due to wakes, using the wind farm case can be seen in table 9, where the logarithmic profile (Z_0 = 0.00055 m) has been used together with the Eddy viscosity wake model. The fully utilized area leads to higher impact of wake effects compared to the partial wind farm case results in table 6. However, the results are not deviating too much from the results of the partial wind farm case using the modified Park wake model in table 8. Furthermore, for the first time the results clearly show that both the 12 MW and the 17 MW turbine layout contribute to greater impact of the wake effects.

Table 9. Loss of electricity production due to wakes for the wind farm case using logarithmic profile (Z_0 = 0.00055 m) and Eddy viscosity wake model.

Separation Distance \ Rated Power	12 MW	16 MW	17 MW
Circular distance 4D		~16.1%	
Elliptical distance 7Dx4D		~10.6%	
Circular distance 7D	~7.2%	~6.2%	~6.7%
Elliptical distance 10Dx7D		~4.9%	
Circular distance 10D		~3.4%	

4.1.4 Electricity Production per Area

The previous results show the impact of wake effects for different layouts. However, the change of distancing and rotor diameter (due to a change in rated power) also impact how well the area is being utilized, as can be seen in table 10. Larger distancing contributes to a less utilized layout, making the electricity produced per unit area smaller. Compared to table 6 it can be seen that higher rated power results in a better utilization of the area, despite leading to higher wake effects. A layout with smaller turbines leads to both larger wake effects and a less utilized area.

Table 10. Electricity production (kWh) per square meter for the partial wind farm case using logarithmic profile (Z_0 = 0.00055 m) and Eddy viscosity wake model.

Separation Distance \ Rated Power	12 MW	16 MW	17 MW
Circular distance 4D		96.9	
Elliptical distance 7Dx4D		61.1	
Circular distance 7D	33.4	35.3	36.1
Elliptical distance 10Dx7D		25.7	
Circular distance 10D		18.2	

4.1.5 Rotor Diameter Sensitivity Analysis

A sensitivity analysis of the rotor diameter for the 16 MW and 7D circular spacing layout can be seen in table 11. The change in impact of wake effect is minimal even for a 20% increase or decrease in rotor diameter. However, the impact of wakes seems to decrease together with a decrease of rotor diameter. It should also be noted that the turbines change position as the rotor diameter is changed, due to the distancing constraint being given in terms of the rotor diameter.

Table 11. Sensitivity analysis of the rotor diameter for the base case using logarithmic profile (Z_0 = 0.00055 m) and Eddy viscosity wake model. The layout used is 16 MW turbines with 7D circular distancing.

Rotor Diameter	**Lost production due to wakes**
199.2 m (-20%)	~4.8%
249.0 m	~4.8%
298.8 m (+20%)	~4.9%

4.1.6 Hub Height Sensitivity Analysis

A sensitivity analysis of the hub height for the 16 MW and 7D circular spacing layout can be seen in table 12. A monotone pattern of lower wake impact with higher hub heights can be seen, which is the opposite pattern of what can be seen in table 11. The opposite behaviour of table 12 compared to table 11 can be the explanation of no clear change of the wake effect impact for turbines with different rated power seen in table 6.

Table 12. Sensitivity analysis of the hub height for the base case using logarithmic profile (Z_0 = 0.00055 m) and Eddy viscosity wake model. The layout used is 16 MW turbines with 7D circular distancing.

Hub Height	**Lost production due to wakes**
139.6 m (-20%)	~5.0%
157.1 m (-10%)	~4.9%
174.5 m	~4.8%
192.0 m (+10%)	~4.8%
209.4 m (+20%)	~4.7%

4.1.7 Site Roughness Sensitivity Analysis

4.1.7.1 Eddy Viscosity

A sensitivity analysis of the site roughness for the 16 MW and 7D circular spacing layout based on the Eddy Viscosity wake model can be seen in table 13. The differences in impact from wake effects are small when using the Eddy viscosity wake model. The impact of wakes seems to be lower for smaller site roughness.

Table 13. Sensitivity analysis of the site roughness for the base case using logarithmic profile (Z_0 = 0.00055 m) and Eddy viscosity wake model. The layout used is 16 MW turbines with 7D circular distancing.

Roughness (Z_0)	**Lost production due to wakes**
0.00020 m (calm sea)	~4.9%
0.00055 m (blown sea)	~4.8%
0.0010 m	~4.8%

4.1.7.2 Modified Park

A sensitivity analysis of the site roughness for the 16 MW and 7D circular spacing layout based on the modified Park wake model can be seen in table 14. For this wake model, the results are more clear where a decrease in site roughness leads to higher wake impact. The resulting impact of wakes is higher when the Park model is used compared to the previous results in table 13, something that has already been seen in section *4.1.2 Wake Model*.

Table 14. Sensitivity analysis of the site roughness for the base case using logarithmic profile (Z_0 = 0.00055 m) and the modified Park wake model. The layout used is 16 MW turbines with 7D circular distancing.

Roughness (Z_0)	**Lost production due to wakes**

0.00020 m (calm sea)	~7.2%
0.00055 m (blown sea)	~6.9%
0.0010 m	~6.6%

4.1.8 Sector Management

The results from the sector management simulations can be seen in Table 15. The results are based on the wind farm layout of 16 MW turbines with 7D circular distancing. It can be seen that performing sector management for the 'first 5 downstream turbines among the worst performing' achieve higher electricity production than performing sector management on the '20 best performing turbines' for the same wind speed range. However, sector management does not result in higher electricity production compared to the initial setup without sector management. Furthermore, it seems that sector management has a less desirable outcome (lower electricity production) when applied to a lower wind speed range.

Table 15. Impact of sector management on the electricity production for different sector setups and wind speed ranges.

Turbines Disabled	**Wind Speed Range** (m/s)	**Resulted Electricity Production** (GWh)	**Share of Initial Electricity Production**
The 20 best performing turbines	2 - 7	4 129.9	~98.3%
The 20 best performing turbines	20 - 25	4 161.5	~99.1%
The 20 best performing turbines	23 - 25	4 194.2	~99.9%
The first 5 downstream turbines among the worst performing	20 - 25	4 191.8	~99.8%
The first 5 downstream turbines among the worst performing	23 - 25	4 198.6	~100%

4.1.9 External Wake from a Neighbouring Cluster

The impact of external wake effects from the neighbouring cluster can be seen in figure 13. It can be seen that the impact of wakes decreases as the distance between the two clusters increases. The distance is measured as the distance to the closest turbine in horizontal direction (including the distancing constraint). The results can be compared to the results of internal wakes for the same base case layout of 16 MW turbines with 7D distancing, which results in ~4.8% lost electricity production. For a distance of 2*L* (17 430 m), the impact contributed to a less than 0.1% reduction of electricity production.

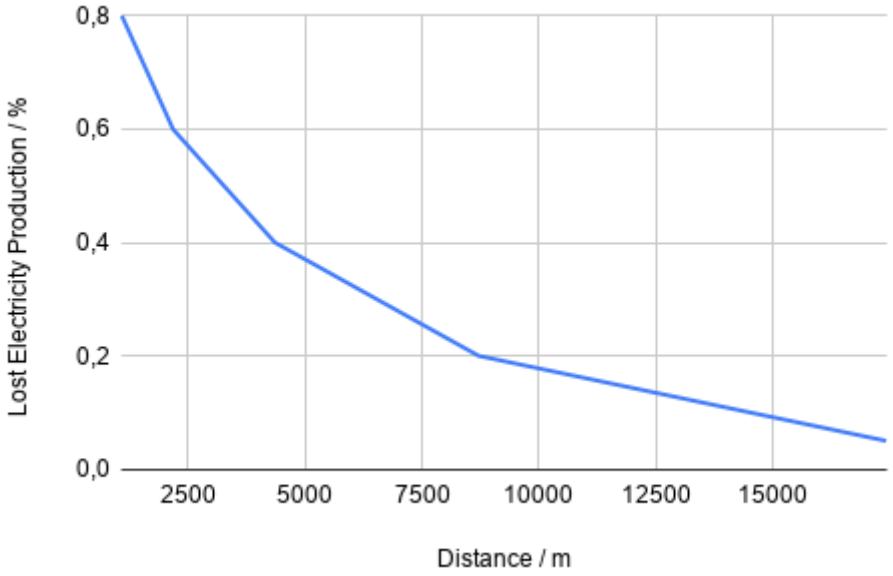

Figure 13. Graph showing the loss of electricity production due to external wakes from a neighbouring cluster as a function of the distance. The result was obtained by using the logarithmic profile (Z_0 = 0.00055 m) and Eddy viscosity wake model (base case). The distance *L* given as the horizontal length of the base case setup (5 turbines including distancing constraints).

4.2 Economic Analysis

4.2.1 Levelized Cost of Electricity

The calculated LCOE for the different wind farm layouts can be seen in table 16. The tendency of lower electricity production with increased distancing due to lower utilization of the area can be seen, as have been shown in table 10. However, the costs are falling as well, making it a bit more economical to choose a wind farm layout with larger distancing.

Table 16. Levelized cost of electricity for different wind farm layouts.

Wind Farm Layout	**Total Costs**	**Electricity Production**	**LCOE**
16 MW Circular distance 7D	2 169 380 745 €	4 199.7 GWh / yr	52.6 € / MWh
16 MW Elliptical distance 10Dx7D	1 499 000 440 €	2 950.6 GWh / yr	51.8 € / MWh
16 MW Circular distance 10D	1 076 226 300 €	2 140.15 GWh / yr	51.2 € / MWh

4.2.1.1 Increased Hub Height

The calculated LCOE for different hub heights can be seen in table 17. The evolution of higher LCOE with increased hub height suggests it is not economical to increase the hub height in order to achieve higher electricity production, based on the wind farm layout with 16 MW turbines and 7D circular distancing. The initial hub height is 174.5 m.

Table 17. Levelized cost of electricity for increased hub heights based on the wind farm case of 16 MW turbines with 7D circular distancing.

Hub Height	**Total Costs**	**Electricity Production**	**LCOE**
184.5 m (+10 m)	2 211 815 520 €	4 225.0 GWh	53.3 € / MWh
194.5 m (+20 m)	2 254 250 290 €	4 249.2 GWh	54.0 € / MWh
204.5 m (+30 m)	2 296 685 060 €	4 271.6 GWh	54.7 € / MWh

5. Discussion

5.1 Discussion of the Results

The wake effect has been seen to be dependent on the separation distance set between the turbines. However, only looking at the impact of wakes with increased distancing does not describe the effect on total electricity production or how well the area is utilized. An increase of the distancing constraint does result in a less utilization of the area as well as a lower LCOE that makes the project more profitable. A lowering of the distancing constraint from 10D to 7D will result in almost a doubling of the electricity production, however with a LCOE price increase of ~2.7%, leaving the decision to be made based on the expectation to produce as much as electricity as possible, or simply just generating the most profitable project.

A change of the rated power of the turbines did primarily not show a clear change of wake effect impact, however it was later shown that an increase of the rotor diameter resulted in higher wake effects while an increase in hub height resulted in lower wake impact, making the opposite relationship cancelling out the combined effect. When simulating the same change of rated power for the wind farm case, both the 12 MW and the 17 MW turbine showed a bigger impact of wakes when keeping the distance constant, concluding that a rated power in between would deliver the most desirable result when focusing on the wakes. However, this may not hold true for other wind farm layouts or hub heights.

The exact impact of wakes could not be easily concluded as the reported impact of wakes could differ between 1.2 and 3.4 percentage points based on which wake model was used. Furthermore, the difference between the estimated wakes for the wind farm case using Eddy Viscosity and the partial wind farm case using modified Park was lower than by simply using the two different wake models for the partial wind farm case scenario, which shows that the choice of wake model could have a bigger impact than if the number of turbines is increased from 20 to over 60 for the same wake model. The choice of site roughness will also impact the estimation of the wake effect, although the biggest difference was 0.3 percentage points for the modified Park model when using values for calm and blown sea.

The resulting wake effect impact from a neighbouring wind farm showed to be of less importance compared to internal wake effects. For the base case layout, the external wakes could contribute to a 0.2% loss of electricity production when the distance to the neighbouring park was 8 715 m, representing the longest horizontal distance between two turbines within the wind farm. When the distance was lowered to 1 084.4 m, representing just ⅛ of the same length, the loss of electricity production due to wakes was 0.8%. Comparing this to the internal wake effect impact of 4.8% loss of production, shows that internal wake is of greater importance. However, the loss of production due to external wakes decreases exponentially with increased separation distance between the two wind farms.

In order for companies to choose to place turbines closer to each other, there would be needed for the company to benefit from focusing on producing as much electricity as possible rather than just focus on profitability. Here, legislators can put pressure on

demanding higher utilization of the area by regulations. Furthermore, regulations could also play a role in guaranteeing that no wind farms will be planned at a certain distance from the existing one, thus limiting the uncertainties experienced by the company in terms of possible loss of electricity production due to external wakes. There is also a possibility for legislators to take a role in the development of all wind farm clusters in the region and thus contributing to an optimization of the region as a whole rather than optimizing each cluster for itself.

5.2 Uncertainties with This Work

In order to predict the future trends there has been a need to base the estimations on a ‘common variable’ in this report meaning that the predicted trend of both rotor diameter and turbine height would be dependent on the rated power. However, this may not hold for all turbine models as individual technical aspects can contribute to either a better or an inferior wind turbine. In other words, there is a spread along the predicted figure and furthermore, the future prediction is based solely on the past trend, opening up for errors in case of a major trendshift that can be caused by technological progress. For the prediction of the rotor diameter, linear regression was used while the prediction for turbine height used ‘four parameter logistic regression’. This regression model contributed to a lower error around the fitted curve, however there is a risk of overfitting that results in an exponential evolution that may not match with the reality.

The wind data has a big impact on the estimated electricity production. The wind data used for the site was not gathered by a local met mast, rather, it was provided by estimated data from the *MERRA-2* database and can therefore be overestimating or underestimating the electricity production, which in turn can impact the resulting wakes (NASA, 2019). Additionally, the wind shear model may not correctly estimate the wind velocity at the given height.

Most of the models for wake effects are based on simple single wake calculations with an assumption of superposition of merging wakes, such as the Katić model (Sørensen, 2011). Also, the models are mainly based on steady-state considerations, and thus disregard the effect of dynamic wakes that have a big impact on wind turbine loadings. Another deficiency in the current simplified models is that they seek to predict the development of the reduced mean velocity, disregarding the properties of turbulence. Therefore, the calculations made with the Modified Park model, that derive reduced wind speeds by the site roughness, may not reflect a completely realistic scenario.

However, calculations in *WindFarmer: Analyst* were mainly done by the Eddy Viscosity wake model that base the calculations on a computational fluid dynamic (CFD) algorithm to calculate wind speeds, energy losses and turbulence (DNV GL, n.d.-b). The Eddy Viscosity wake model is still a simplified CFD model but unlike the Modified Park model, this wake model does not assume undistributed atmospheric flow and therefore doesn't overlook the impact of field flow. Still, trying to model wakes using field measurements instead, comes with its own setbacks (Sørensen, 2011). This is mainly due to the complicated and ever-changing inflow conditions. All conditions may not be fully known and uncertainties can arise due to a lack of stationary data.

The economic analysis is heavily dependent on the choice of turbine layout as well as the cable layout. In addition, the costs were mainly based on course material that are not provided by a real manufacturing company. It should be noted that no real price offerings exist for the 16 MW and 17 MW turbine as they do not exist today, and that the real price offering of the 12 MW turbine is subject to change as it gets adopted by the broader market.

6. Conclusions & Future Work

The results of this work has shown the importance of considering the wake effect for future offshore wind farm development. For clusters containing 20 turbines (16 MW), the lost electricity production due to wakes have been shown to stand for 4.8% of the gross yield when using 7D separation distance and Eddy Viscosity wake model. For wakes considered within the wind farm, the same settings contributed to a loss of electricity production representing 6.2% of the gross yield. The biggest impact was obtained for the wind farm case of 16 MW turbines with 4D separation distance, which resulted in a 16.1% loss of electricity production relative to the gross yield. Layout changes that were introduced in order to mitigate the impact of wakes, such as smaller rotor diameter and higher towers, showed modest improvements within the range of tenths of a percentage point. Other measures, such as sector management, resulted in a less desirable outcome. In the case of building neighbouring wind farm clusters (with a distance of ~3 km), the impact would be another 0.5 percentage points loss in electricity production relative to the gross yield. Therefore, a major conclusion with this work is that the relative distance between turbines within the wind farm cluster has the biggest impact on wakes. Using larger distancing constraints within the farm has been shown to be more profitable, with a ~2.7% lower LCOE for 10D distancing compared to 7D distancing, however with a lower electricity production in total.

The following areas may be of interest for future research in connection to the subject of this thesis:

- More research can be done on wake effect mitigation by using yaw control & sector management. Other mitigation measures can include a variability of the height within the wind farm.

- More research can be done on how to mitigate the negative wake impact due to bigger rotors.

- Larger towers entails lower impact from wakes and further work should be done on the possibility of further increasing the hub height. This includes both the technology and lowering the costs in order to make such changes profitable.

- Research in developing more accurate CFD modelling would help limit the uncertainties, as the model is of big importance for estimating the wake effect.

- Furthermore, there is a need to evaluate the balance between wake mitigation and maximum electricity production, as the latter shows to be less profitabile.

References

Ainslie, J. F. (1988). Calculating the flowfield in the wake of wind turbines. *Journal of Wind Engineering and Industrial Aerodynamics*, Volume 27, Issues 1–3, pp. 213-224, ISSN 0167-6105. https://doi.org/10.1016/0167-6105(88)90037-2.

Aldersey-Williams, J. Rubert, T. (2019). Levelised cost of energy – A theoretical justification and critical assessment, *Energy Policy*, Volume 124, pp. 169-179, ISSN 0301-4215, https://doi.org/10.1016/j.enpol.2018.10.004.

Aspliden, C. I., Elliot, D. L. and Wendell, L. L. (1986). Resource Assessment Methods, Siting, and Performance Evaluation. In: R. Guzzi and C. G. Justus. (eds.) *Physical Climatology for Solar and Wind Energy*. New Jersey, World Scientific.

Avdic, D. B. Ståhl, P. (2019). Baltic InteGrid review: towards a meshed offshore grid in the Baltic Sea. Baltic InteGrid. http://www.baltic-integrid.eu/index.php/download.html.

Baltex Power S.A. (2011). *Havsbaserad vindkraftspark Norra Östersjön. Projektets informationskort*. Available at: https://www.ym.fi/download/noname/%7B014866E5-7928-4EAE-940B-5270ED6AB8E5%7D/32350.

Beaucage, P. Brower, M. Robinson, N. Alonge, C. (2012). Overview of six commercial and research wake models for large offshore wind farms. In: *Proceedings of the EWEA Conference*. Copenhagen, Denmark. https://citeseerx.ist.psu.edu/viewdoc/download?doi=10.1.1.467.3903&rep=rep1&type=pdf.

Betz, A. (1919). Schraubenpropeller mit geringstem Energieverlust. Dissertation, Göttingen. Nachrichten, Göttingen

Brand, A. J. (2009). The effect of wind farming on mesoscale flow - Validation and prediction. ECN Wind Energy. https://publications.tno.nl/publication/34631107/8Anw90/m09051.pdf

Burton, T., Sharpe, D., Jenkins, N., Bossanyi, E. (2001b). The Wind Resource. In: *Wind Energy Handbook.* Chichester, John Wiley and Sons. pp. 18-20.

DNV GL. (n.d.-a). *WindFarmer - Wind farm design software*. Available at: https://www.dnvgl.com/publications/windfarmer-wind-farm-design-software-43047. [Accessed: 20th January 2021]

DNV GL. (n.d.-b). *WindFarmer: Analyst maximizes your wind energy production assessment capability with a step by step process*. Available at: https://www.dnvgl.com/software/software-services/windfarmer-analyst-features.html. [Accessed: 3rd January 2021]

Eriksson, O. (2019). Numerical Computations of Wakes Behind Wind Farms: A tool to study Farm to Farm interaction. *Digital Comprehensive Summaries of Uppsala Dissertations from the Faculty of Science and Technology*. Uppsala, Acta Universitatis Upsaliensis. p. 73. ISSN 1651-6214.

European Commission. (2019). *Renewable Energy – Recast to 2030 (RED II)*. Available at: https://ec.europa.eu/jrc/en/jec/renewable-energy-recast-2030-red-ii. [Accessed: 7th November 2020]

EWEA (The European Wind Energy Association). (2009). Wind Farm Design. In: *Wind Energy - The Facts.* London, Earthscan Publications Ltd. pp. 51-99.

GE Renewable Energy. (n.d.). *Haliade-X offshore wind turbine. The world's most powerful offshore wind turbine in operation*. Available at: https://www.ge.com/renewableenergy/wind-energy/offshore-wind/haliade-x-offshore-turbine. [Accessed: 10th December 2020]

Hansen, K. S. Réthoré, P-E. Palma, J. Hevia, B. G. Prospathopoulos, J. Peña, A. Ott, S. Schepers, G. Palomares, A. van der Laan, M. P. Volker, P. (2015). Simulation of wake effects between two wind farms. *Journal of Physics: Conference Series.* Vol 625. https://doi.org/10.1088/1742-6596/625/1/012008.

Hsu, S. A. Meindl, E. A. Gilhousen, D. B. (1994). Determining the Power-Law Wind-Profile Exponent under Near-Neutral Stability Conditions at Sea. *Journal of Applied Meteorology and Climatology 33*, vol. 6, pp. 757-765, https://journals.ametsoc.org/view/journals/apme/33/6/1520-0450_1994_033_0757_dtplwp_2_0_co_2.xml.

Hüffmeier, J. Goldberg, M. (2019). *Offshore Wind and Grid in the Baltic Sea – Status and Outlook until 2050*. Swedish Agency for Marine and Water Management (SwAM), Research Institutes of Sweden (RISE).

IRENA (International Renewable Energy Agency). (2019). *FUTURE OF WIND. Deployment, investment, technology, grid integration and socio-economic aspects*. Available at: https://www.irena.org/-/media/Files/IRENA/Agency/Publication/2019/Oct/IRENA_Future_of_wind_2019.pdf.

IRENA (International Renewable Energy Agency). (n.d.). *Wind energy.* Available at: https://www.irena.org/wind. [Accessed: 27th December 2020]

Jensen, N. O. (1983). *A note on wind generator interaction*. Risø National Laboratory. Risø-M, No. 2411

Kullberg, M. (2011). *Vindkraftprojekt Södra Midsjöbanken. Samrådsunderlag*. E.ON. Available at: https://ym.fi/documents/1410903/38439968/Sodra-Midsjobanken_samradsunderlag-83F41508_D131_4AA6_A3BE_111C13660C0A-32601.pdf/6ca12b6d-b44c-043d-94be-b617e632e8

1c/Sodra-Midsjobanken_samradsunderlag-83F41508_D131_4AA6_A3BE_111C13660C0A-32601.pdf?t=1603262312627.

Manwell, J. F. McGowan, J. G. Rogers, A. L. (2009). *Wind energy explained. Theory, design and application.* Second edition. Chichester, John Wiley and Sons.

Molina, M. Mercado, P. (2011). *Modelling and Control Design of Pitch-Controlled Variable Speed Wind Turbines*. https://doi.org/10.5772/15880.

NASA (National Aeronautics and Space Administration). (2019). *Modern-Era Retrospective analysis for Research and Applications, Version 2.* Available at: https://gmao.gsfc.nasa.gov/reanalysis/MERRA-2/. [Accessed: 20th January 2021]

Naturvårdsverket. (2020). *Baltica 1 - polsk vindkraft Midsjöbanken*. Available at: https://www.naturvardsverket.se/Stod-i-miljoarbetet/Remisser-och-Yttranden/Remisser/Planer-i-vara-grannlander---Esbokonventionen/Baltica-1-polsk-vindkraft-Midsjobanken/. [Accessed: 7th November 2020]

Peña, A., Réthoré, P. E., van der Laan, M. P. (2015). On the application of the Jensen wake model using a turbulence‐dependent wake decay coefficient: the Sexbierum case. *Wind Energy.* Volume 19, Issue 4, pp. 763-765. https://doi.org/10.1002/we.1863.

Svensson, J. (2019). Course material. Wind Power Systems EIEN10. Lund University, Faculty of Engineering.

Sørensen, J. N. (2011). 4 - Wind turbine wakes and wind farm aerodynamics. In: Sørensen, J. D. Sørensen, J. N. (eds.) Wind Energy Systems. *Woodhead Publishing Series in Energy*. pp. 112-e131, ISBN 9781845695804, https://doi.org/10.1533/9780857090638.1.112.

Tillväxtanalys. (2014). *Politik för ett hållbart energisystem i Polen.* Available at: https://www.tillvaxtanalys.se/download/18.62dd45451715a00666f205e1/1586366205265/Energisystem+bortom+2020+Polen.pdf. [Accessed: 7th November 2020]

Tong, W. (2010). *Wind Power Generation and Wind Turbine Design*. Southampton, WIT Press.

UK government. (2020). *Policy paper. Offshore wind Sector Deal.* Available at: https://www.gov.uk/government/publications/offshore-wind-sector-deal/offshore-wind-sector-deal. [Accessed: 10th December 2020]

Vermeer, L. J., Sørensen, J. N., Crespo, A. (2003). Wind turbine wake aerodynamics, *Progress in Aerospace Sciences*, Volume 39, Issues 6–7, pp. 467-510, ISSN 0376-0421, https://doi.org/10.1016/S0376-0421(03)00078-2.

Appendices

Appendix 1

Size evolution of wind turbines over time (Molina & Mercado, 2011). (*) Note that the data for 2015 was a prediction at the time of the study.

	1990	1995	2000	2005	2010	2015*
Installed power	0.5 MW	1.3 MW	2 MW	4.5 MW	7 MW	10 MW
Rotor diameter	40 m	70 m	80 m	120 m	126 m	145 m

Appendix 2

Evolution of wind turbine height over time (UK government, 2020; GE Renewable Energy, n.d.).

	2002	2014	2018	2020
Installed power	2 MW	6 MW	8.5 MW	12 MW
Turbine height	93 m	180 m	200 m	260 m

Appendix 3

WGS84 coordinates of the *MFW Baltyk Północny* wind farm boundary area (Baltex Power S.A., 2011).

	Longitude			Latitude		
	°	‘	‘’	°	‘	‘’
A	17	08	5,9219	55	31	45,3848
B	17	22	48,0842	55	35	12,9062
C	17	24	39,0031	55	35	46,6414
D	17	24	4,8218	55	33	34,4386
E	17	25	18,6708	55	31	52,4230
F	17	24	30,7190	55	28	28,3090
G	17	23	21,1507	55	28	58,3008
H	17	11	27,7087	55	28	43,9310
I	17	08	45,0747	55	29	53,4755

Appendix 4

UTM coordinates used for the wind farm boundary area in *WindFarmer: Analyst*.

	Latitude (mE)	Longitude (mN)
A	634761.8	6155773.2
B	650003.3	6162674.5
C	651895.2	6163793.7
D	651442.2	6159690.2
E	652854.5	6156572.6
F	652241.6	6150230.8
G	650989.2	6151110.1
H	638465.6	6150257.4
I	635561.1	6152335.8

Appendix 5

Turbine specifications for Generic Turbine 3.0 MW.

Wind speed (m/s)	Power output (kW)	Thrust coefficient
0	0	0
1	0	0
2	0	0.1
3	4	0.65
4	60	0.97
5	200	0.99
6	400	0.95
7	640	0.9
8	940	0.85
9	1440	0.78
10	2000	0.72
11	2680	0.6
12	3000	0.5
13	3000	0.4
14	3000	0.3

Appendix 6

Turbine specifications for Generic Turbine 12.0 MW Extrapolated.

Wind speed (m/s)	Power output (kW)	Thrust coefficient
0	0	0
1	0	0
2	0	0.1
3	16	0.65
4	240	0.97
5	800	0.99
6	1600	0.95
7	2560	0.9
8	3760	0.85
9	5760	0.78
10	8000	0.72
11	10720	0.6
12	12000	0.5
13	12000	0.4
14	12000	0.3

15	3000	0.25
16	3000	0.2
17	3000	0.15
18	3000	0.12
19	3000	0.09
20	3000	0.08
21	3000	0.07
22	3000	0.06
23	3000	0.05
24	3000	0.05
25	3000	0.05

15	12000	0.25
16	12000	0.2
17	12000	0.15
18	12000	0.12
19	12000	0.09
20	12000	0.08
21	12000	0.07
22	12000	0.06
23	12000	0.05
24	12000	0.05
25	12000	0.05

Appendix 7

Turbine specifications for Generic Turbine 16.0 MW Extrapolated.

Wind speed (m/s)	Power output (kW)	Thrust coefficient
0	0	0
1	0	0
2	0	0.1
3	21.36	0.65
4	320	0.97
5	1064	0.99
6	2136	0.95
7	3440	0.9
8	5040	0.85
9	7680	0.78
10	10640	0.72
11	14320	0.6
12	16000	0.5
13	16000	0.4
14	16000	0.3
15	16000	0.25
16	16000	0.2
17	16000	0.15
18	16000	0.12
19	16000	0.09

Appendix 8

Turbine specifications for Generic Turbine 17.0 MW Extrapolated.

Wind speed (m/s)	Power output (kW)	Thrust coefficient
0	0	0
1	0	0
2	0	0.1
3	22.695	0.65
4	340	0.97
5	1130.5	0.99
6	2269.5	0.95
7	3655	0.9
8	5355	0.85
9	8160	0.78
10	11305	0.72
11	15215	0.6
12	17000	0.5
13	17000	0.4
14	17000	0.3
15	17000	0.25
16	17000	0.2
17	17000	0.15
18	17000	0.12
19	17000	0.09

20	16000	0.08
21	16000	0.07
22	16000	0.06
23	16000	0.05
24	16000	0.05
25	16000	0.05

20	17000	0.08
21	17000	0.07
22	17000	0.06
23	17000	0.05
24	17000	0.05
25	17000	0.05

Appendix 9

Specifications of the flow field boundary used for the flow model setup.

Topological Sensitivity	North West - X	North West - Y	X Width	Y Width	Resolution
0.001	630197.5	6166527.6	30040.5	17951.1	100

Appendix 10

UTM coordinates of the first (bottom right corner) turbine for different layouts (wind farm case).

Wind Farm Layout	**Coordinate - X**	**Coordinate - Y**
16 MW Circular distance 4D	651792	6151230
16 MW Elliptical distance 7Dx4D	651056	6151227
16 MW Circular distance 7D	651479	6151159
16 MW Elliptical distance 10Dx7D	650765	6151232
16 MW Circular distance 10D	651164	6151159
12 MW Circular distance 7D	651479	6151159
17 MW Circular distance 7D	651436	6151159

Appendix 11

Specific coordinates for turbines deviating from the symmetrical placing. The layout is based on 16 MW turbines with 4D circular spacing (wind farm case).

Name	Coordinate - X	Coordinate - Y
Turbine 59	650775.6	6162957.1
Turbine 60	651744	6163555
Turbine 61	651600	6162200

Appendix 12

Specific coordinates for turbines deviating from the symmetrical placing. The layout is based on 16 MW turbines with 7D x 4D elliptical spacing (wind farm case).

Name	Coordinate - X	Coordinate - Y
Turbine 2	652123.2	6150495.8
Turbine 12	649702.7	6161530.3
Turbine 14	647916.5	6161520.8
Turbine 59	650323.7	6162656.8
Turbine 60	651744	6163555

Turbine 61	651553.3	6162115.8

Appendix 13

Specific coordinates for turbines deviating from the symmetrical placing. The layout is based on 16 MW turbines with 7D circular spacing (wind farm case).

Name	Coordinate - X	Coordinate - Y
Turbine 58	651425	6160685
Turbine 59	648575	6161884
Turbine 60	651744	6163555
Turbine 61	650513.2	6162300

Appendix 14

Specific coordinates for turbines deviating from the symmetrical placing. The layout is based on 16 MW turbines with 10D x 7D elliptical spacing (wind farm case).

Name	Coordinate - X	Coordinate - Y
Turbine 3	651445.5	6161303.8
Turbine 16	651727.2	6163523.2
Turbine 19	649609.8	6162317.5

Appendix 15

Specific coordinates for turbines deviating from the symmetrical placing. The layout is based on 16 MW turbines with 10D circular spacing (wind farm case).

Name	Coordinate - X	Coordinate - Y
Turbine 11	651740	6163550
Turbine 12	649500	6162300

Appendix 16

Specific coordinates for turbines deviating from the symmetrical placing. The layout is based on 17 MW turbines with 7D circular spacing (wind farm case).

Name	Coordinate - X	Coordinate - Y
Turbine 58	651436	6161250
Turbine 60	651744	6163555

Appendix 17

Specific coordinates for turbines deviating from the symmetrical placing. The layout is based on 12 MW turbines with 7D circular spacing (wind farm case).

Name	Coordinate - X	Coordinate - Y
Turbine 73	651565	6161831
Turbine 74	648760	6161985

Turbine 61	650000	6162520

Turbine 75	651760	6163580
Turbine 76	650161	6162635

Appendix 18

Proposed cable layout for 16 MW turbines with 7D circular spacing (wind farm case). Blue lines representing the 185 mm^2 cable. Black lines representing the 400 mm^2 cable. Transformers marked with stars with the one to the left representing the 432 MW transformer and the one to the right representing the 544 MW transformer.

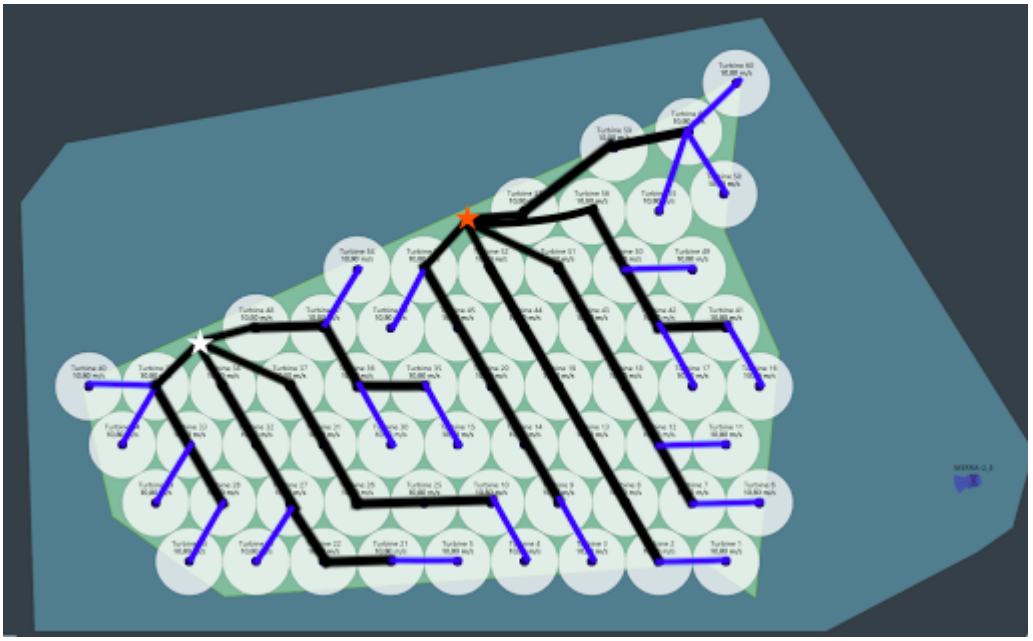

Appendix 19

Proposed cable layout for 16 MW turbines with 10D x 7D elliptical spacing (wind farm case). Blue lines representing the 185 mm^2 cable. Black lines representing the 400 mm^2 cable. Transformers marked with stars with the one to the left representing the 336 MW transformer and the one to the right representing the 336 MW transformer.

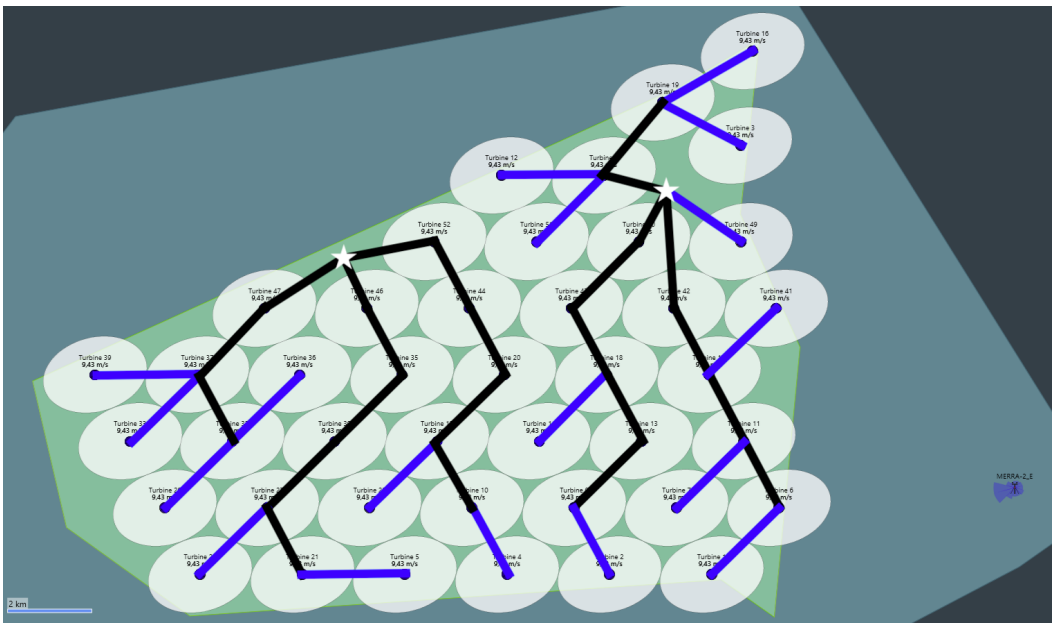

Appendix 20

Proposed cable layout for 16 MW turbines with 10D circular spacing (wind farm case). Blue lines representing the 185 mm^2 cable. Black lines representing the 400 mm^2 cable. Transformers marked with stars with the one to the left representing the 208 MW transformer and the one to the right representing the 272 MW transformer.